THE EFFECT OF LINEAR GUIDE REPRESENTATION FOR TOPOLOGY OPTIMIZATION ON A FIVE-AXIS MILLING MACHINE

by

ESRA YÜKSEL

Submitted to the Graduate School of Engineering and Natural Sciences

in partial fulfillment of the requirements for the degree of
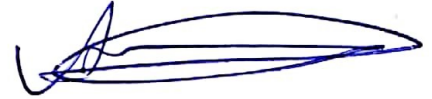
Master of Science

Sabancı University

2017

THE EFFECT OF LINEAR GUIDE REPRESENTATION FOR TOPOLOGY OPTIMIZATION ON A FIVE-AXIS MILLING MACHINE

Approved by:

Prof. Dr. Erhan Budak (Thesis Supervisor)

Prof. Dr. Ata Muğan

Assist. Prof. Lütfi Taner Tunç

Date of approval:

28. 07. 2017

To Ebru &Nurhan.

THE EFFECT OF LINEAR GUIDE REPRESENTATION FOR TOPOLOGY OPTIMIZATION ON A FIVE-AXIS MILLING MACHINE

Esra Yüksel

Manufacturing Engineering, MSc. Thesis, 2017

Thesis Supervisor: Prof. Dr. Erhan Budak

ABSTARCT

Topology optimization is a countermeasure to obtain lightweight and stiff structures for machine tools. Topology optimizations are applied at component level due to computational limitations, therefore linear guides' rolling elements are underestimated in most of the cases. Stiffness of the entire assembly depends on the least stiff components which are identified as linear guides in the current literature. In this study, effects of linear guide's representation in virtual environment are investigated at assembly level by focusing on topology optimization. Two different contact models are employed for rolling elements in the linear guides. Reliability of the contact models are verified with experiments. After the verification, heavy duty cutting conditions are considered for the system and topology optimization is performed for two different contact models to reduce the mass of the structure. The difference caused by the representation of rolling elements is demonstrated for the same topology algorithm and the optimization results are compared for the models. And then, the effect of using stiffer linear guides in the five-axis milling machine is investigated by increasing the stiffness of the contact elements. Afterwards, an extensive Multiple-Physics comparison for different linear guide's representations is executed for dynamically and thermally by crossing the representations for the proposed structures. As first, dynamic behavior improvement and error percentage due to unrealistic representation is investigated, while thermal behavior is investigated as the second. As the last, it is demonstrated that minimum compliance problem contributes

dynamic and thermal stiffness with realistic boundary conditions for multi-component level topology optimization applications

MASURALI LİNEER RULMANLARIN SANAL TEMSİLİNİN BEŞ-EKSEN FREZE MAKİNASININ TOPOLOJİ OPTİMİZASYONU ÜZERİNE ETKİSİ

Esra Yüksel

Üretim Mühendisliği, Yüksek Lisans Tezi, 2017

Tez Danışmanı: Prof. Dr. Erhan Budak

ÖZET

Topoloji optimizasyonu hafif ve rijit takım tezgâhı yapıları elde etmek için temel bir kilometre taşı olarak nitelendirilebilir. Topoloji optimizasyonu uygulamaları, ağır hesaplama yükü yüzünden çoğu zaman, lineer rulman sistemlerinin dönel masuraları ya da bilyeleri ihmal edilerek yapılır. Tüm tezgâhın rijitliği ise montaj içerisindeki en az rijit olan elemanlara bağlıdır ki bunlar mevcut literatürde lineer rulman sistemleri olarak belirtilmektedir. Bu çalışmada, lineer rulman sistemlerinin sanal ortamdaki gösterimi, montaj seviyesindeki topoloji optimizasyonu uygulamaları için incelenmiştir. İki farklı kontak modeli masuralı lineer rulman sistemleri için incelenmiştir. Kontak modellerinin güvenilirliği deneylerle test edilmiştir. Doğrulama sürecinden sonra, her iki lineer rulman modeline yönelik ağır-iş kesme durumu, takım tezgâhının sanal simülasyonu ve topoloji optimizasyonu ile kütle çıkarılması için temel alınmıştır. Optimizasyon için aynı algoritma kullanılmasına rağmen, iki optimizasyon arasındaki farklılık lineer rulmanların dönel elemanlarının sanal ortamda farklı olarak temsil edilmesinden kaynaklanır. Daha sonra, daha rijit lineer rulman sistemlerinin kullanımının yapısal etkisi, dönel rulman elemanlarının rijitliği artırılarak araştırılmıştır. Bundan sonra, kapsamlı çoklu faz fizik etkileşimi karşılaştırması, sanal lineer rulman temsillerini çaprazlayarak dinamik ve termal olarak yapılmıştır. İlk olarak, gerçekçi olmayan lineer rulman temsili için hata oranı ve gerçekçi lineer rulman gösterimi için dinamik iyileşme oranları araştırılmıştır.

İkincil olarak, aynı durum termal davranış için araştırılmıştır. Son olarak topoloji optimizasyonu için enerji temelli minimum esneklik probleminde sınır koşullarının çok önemli olduğu ve bunlarının doğru gösteriminin dinamik ve termal rijiditeye de katkı yapmış olduğu kanıtlandı.

ACKNOWLEDGMENT

This thesis is dedicated to my family and friends. I appreciate all of their support and encouragement while preparing this thesis. I would like to thank my supervisor Prof. Erhan Budak for his support, encouragement, guidance and advise to solve the problems that I faced throughout this thesis.

I wish to thank Prof. Ata Mugan and Dr. Emre Özlü for their vision, help and support. In addition, I want to thank Ahmet Semih Ertürk, Milad Azvar, and all the other MRL members for their support and guidance.

August 2017   Esra YÜKSEL

                                                            (Mechanical Engineer)

TABLE OF CONTENTS

LIST OF FIGURES

LIST OF TABLES

LIST OF SYMBOLS

φ : Compliance

ρ : Density

ρ_e : Elemental density

ρ_{min} : Minimum artificial density

V^* : Admissible Volume

v_e : Elemental volume

g_i^* : Displacement constraint

U : Displacement matrix

F : Force matrix

K : Stiffness matrix

F_R : Roller force

F_{esp} : Experimental total force for a linear guide

R : Number of rollers

δ_N : Normal deflection

δ_{exp} : Experimental deflection

Q : Contact force

K_h : Hertz constant

K_n : Normal stiffness

K_{FE_spring} : Spring stiffness

S : Spring number

Chapter 1 **INTRODUCTION**

Over the last two decades, energy efficient machine tools and lightweight design have become an essential requirement due to competition in the market. To be a survivor and a strong rival, machine tool producers have to provide productive, precise and accurate machines with low costs. Hence, to be able to achieve mentioned specifications, lightweight and stiff structural designs are required. In the current literature, there are two strategies for lightweight design creation.

The first approach is employing lightweight materials with lightweight system mechatronics [1, 17].The lightweight material examples are titanium alloys, metal foam or reinforced polymers such as carbon-fiber polymers and polymer concentrate materials. Also usage of hybrid materials is common, the most known hybrid material is metal-foam sandwich [1].By employing this strategy, up to ~50% mass reduction is possible [18, 19].

The latter approach is structural topology optimization at early design stage. According to material density based topology optimization (Microstructure technique), the objective should be mass reduction while increasing stiffness for machine tool structures [2,5].By help of topology optimization, areas which are not required according to given specifications are removed from the given design domain. Use of this technique requires realistic virtual models and computational power at the same time. Also the employed optimization algorithm and sensitivity filters are vital for the last design proposal [2]. Up to ~30% mass reduction is possible by using topology optimization [1]. The superior side of topology optimization is its

cost. It is significantly cheap compared to the first approach. Therefore, the second approach is the dominant one in the machine tool industry.

The energy efficiency gain is not only mass reduction for the lightweight machine tool structures. Mass reduction comes with a lot of benefits for the other subsystems. The major advantage effect can be seen on servo drives for lightweight machine tools. The existing servo drives can be used at top of energy efficiency limits and the drive bandwidths can be easily extended with mass reduction. The reasons for that can be explained as follows, firstly heavy components give reason to heavy weight forces and the friction losses depend on these weight forces. Lightweight design reduces these friction losses directly [21].As second, accelerating components requires less drive forces/ torques with mass reduction, hence the reactive energy amount of each axis drops. Thus, electrical energy losses reduce due drop at reactive energy amount [1, 21].

Mass reduction and stiffness increase at the same time improve acceleration potential for each axis. This result is significantly important when it combines with stiffness increase for machine tools, because axial velocity, acceleration and jerk saturation limits extend for each axis. Therefore, lightweight machine tool designs are able to reach higher velocities compared the massive ones with same servo driver. Also their acceleration and jerk saturation limits improve significantly. The increase at these saturation limits also means that better product surface quality especially for high speed machining applications. Because when the machine reaches the acceleration and jerk limits during HSM applications, there might be discontinuities due to saturation and this condition might be result with poor surface quality for products [22]. All of the mentioned improvements means that, less machining time is required to manufacture a product for lightweight design structures. In other words productivity increase for machine tool and the same servo drive [1, 20].Theoretically, 30% mass reduction results with 17% productivity increase according to EU Eco-design Directive Standards [20].

Additionally, lightweight machine tool structures enable better process stability due to mass reduction and stiffness increase. Furthermore, lightweight machine tool structures push the

low modes to higher frequencies allowing higher gains to be used in the control loops [23]. Because, first natural frequencies of structural modes and servo drives modes are in a similar bandwidth and they are directly affected from each other [1]. Therefore, the velocity gain which is main parameter for defining drive bandwidth, increases proportional to structural natural frequency. After this augmentation, the position gain is adjusted linearly according to velocity gain. Thus, the servo drive bandwidth extends and it can be used at top of efficiency limits.

To sum up, lightweight design of machine tool structures is mainstreamed for energy efficiency, but it is also important to note that the ability to reach the upper limits of servo drives is another major contributor while developing efficient machine tools. To be able to benefit from this double gain, lightweight materials with adaptive mechatronics or structural topology optimization methodology can be chosen. Most of the well-known machine tool producers prefer the first option at component level although it is more expensive, or they produce massive structures for extreme applications. The reason for that, the structural topology optimization application requires a great engineering infrastructure and computational effort. It requires exact objectives, boundary conditions and realistic FE models at really early design stage. Additionally, most of the topology optimization algorithms are not includes contact parameters, also the design proposal changes for different design objectives and filters. In the current literature, as assembly level topology optimization applications are too rare. Therefore, it is a risky application for manufacturers. But if the structural topology optimization for machine tools would became a reliable design process with scientific researches and developments, it would be the first choice by considering the manufacturing costs. Thus, this thesis is dedicated to contribute topology optimization design methodologies specific to machine tools.

1.1 State of the Art

The current trends and latest advances in machine tool's structural topology optimization is presented within this chapter.

Today, lightweight design of machine tool structures is mainstreamed for energy efficiency, but it is also important to note that the ability to reach the upper limits of servo drivers is another major contributor while developing efficient machine tools. However, to be able to design such a machine tool is not an easy task. Lightweight machine tool structures provide extended working bandwidths for servo drivers compared to the massive ones due to mass reduction. Also, these lightweight structures push the low modes to higher frequencies allowing higher gains to be used in the control loops. The first natural frequencies of lightweight machine tool structures and the drivers are in a similar bandwidth. Therefore, a greater risk may occur during design stage for overlapped modes at low frequencies [1]. In order to overcome the mentioned drawbacks, the everlasting objective should be increasing stiffness globally while reducing or keeping the same component weights [2]. However, entire machine structure stiffness depends on the weakest components of assembly which are usually linear guides and bearings [3, 4].

Topology optimization is one of the most powerful tools for designing lightweight and stiff structures at the early design stage; however, it has its own drawbacks. A typical topology optimization application is carried out in virtual environment by employing FE models of the machine. These models have proved their suitability and significance for subsystem level design analyses such as modeling of ball-screw feed-drive systems [5], spindles [6] and full machine assembly design analyses. However, FE analyses of full machine models are computationally costly. For instance, an FE model of typical machine assembly has one million degrees of freedom (DOF) or more [7]. In order to reduce DOF and model complexity, most of the FE models ignore contact elements and connection parameters. In reducing computational cost, two approaches are common. The first one is to define critical structural components and optimize topology for these components separately. The second is to use the full assembly model for topology optimization with co-FEM or Model Order Reduction techniques [5, 7].

The first approach -defining critical parts and optimizing them- has generally been applied when different considerations are taken into account for topology optimization. In a machine

tool structural optimization problem, the objective might not only be the static stiffness; the end user may also care about chatter and surface quality of the workpiece. Hence, the problem statement must also include dynamic rigidity concerns, and therefore employing a soft-kill BESO method [8] proposed for the component or sub-assembly level. For most practical design problems, 'self –weight' and 'design depended loading' issues drive the objective as minimizing mass while satisfying stress constraints. Due to stress singularity in the computational process reaching a global optimum for a stress-based topology optimization is not guaranteed, therefore it is applied locally [9]. Additionally, it is well known that continuous topology optimization problem forms like SIMP and RAMP methods tend to offer composite material structure in terms of element density [2, 10]. At this point manufacturability is the greatest obstacle for the stiffness objective, although most dominant topology optimization software have casting, drawing and extrusion constraints with the help of MMA methods [11]. Manufacturing constraints pose innumerable computational effort therefore, these constraints strictly limits the assembly optimization initiatives [12].

The second approach- entire assembly optimization - gives superior results while simulating real behavior of the machine tool structure, by representing the contact interfaces. However, simulation of full FE model, is a really time consuming process and is inefficient for a FE solver [7]. Therefore, CMS and Model Order Reduction techniques are applied together [13]. Also co-FEM methods like Multi Body Simulation techniques are coupled with topology optimization to decrease the computational cost [3, 14].

The rolling elements of linear guides have rarely been simulated in a FE model of milling machine assembly until now, due to the computational limitations. Besides, the design tendency for stiff structures have directed designers to create massive structures without considering the least stiff components of the machine tool assembly. Therefore, topology optimization studies for entire machine tool structures by including contact and joint elements are very few. Additionally, the static stiffness, dynamic and thermal characteristics also have an organic connection with the design of the machine tools' structural elements and as well as joints connecting the structural members and machine elements [24, 25]. Mutual

interaction between characteristic and evaluative factors of machine-tool dynamics generally occurs in a competitive and cooperative way between them. Thus, the relationship between design variables, evaluative factors and their solution methodologies become very complicated. If these complicated relations are not well stated and clarified before the formulation of the design optimization problem, the possibility of a poor convergence to a local optimum or the risk of suffering from ill-posed problem is very high, and it is generally not easy to get a design solution with a remarkable upgrade on the product performance [2, 25]. Moreover, number of design variables for machine-tool structures is enormous. Therefore, use of mathematical programming methods is a really difficult to determine all the design variables simultaneously at the same time.

Heretofore, maximum stiffness is considered as the objective and rolling elements mentioned as the most flexible elements as the boundary conditions within the given design domain for machine tool structures. These roller element's mutual effect on a machine tool structure is significant for the stiffness considerations. Static and thermal displacements and dynamic behavior of the entire structure can be taken as a subset of these stiffness considerations at early design stage. It is an advantage for machine tool design from topology optimization view, because energy principles represent the basis of topology optimization of discrete and continuum structures [2, 4, 25].

The stiffness problem equals to design with minimum compliance defined, is basically equivalent to minimizing the total elastic energy at the equilibrium state of the structure. Luckily, these elastic energy equations are consistent with minimization static displacement and thermal deformations and maximization of a single eigenvalue mode. Nevertheless, to be able to connect the direct links between specific proofs of existence for such coupled problems have yet to be discovered. But, to put them into a consistent form, microstructure or macrostructure lay-out (topology optimization) techniques are required. The main disparity between Material or Micro-structure approaches and Geometrical or Macro-structure approaches is the determination method and algorithms of the final layout of the given design domain [26]. By the way, for the Macro-structure approach: the structural

14

topology can be changed by degenerating and/or growing a structure or by inserting holes in a structure while the material approach always finishes with material removal. Therefore, most of the cases Macro-structure techniques are associated with sizing and shape optimization in the literature and it is originated from material techniques.

The strong and superior side of material or Micro-structure techniques is that, it introduces material models which are artificial but compatible with real isotropic materials that can be controlled by an algorithm and allow the density of material to cover the complete range of values from void over to solid as the employed algorithms results. The material distribution methodology as the basis of the microstructure techniques first introduced by Bendsøe & Kikuchi in 1988 [27].Additionally, Kikuchi offered a homogenization technique to be able to obtain a well-posed problem and according to the technique: a tiny cell structure is designed using a fixed grid FE representation and then homogenization is employed to calculate the efficient properties of a material composed of the individual cells [28]. Tenek & Hagiwara employed the homogenization techniques to maximize a single Eigen frequency of both isotropic and composite plates and used SLP to perform the optimization [29]. After many contributions the literature, in 1999 'Solid Isotropic Microstructure with Penalty material' or its known as 'The artificial' or 'The fictitious' material model or 'Interpolation scheme' in the literature presented and developed by Bendsøe & Sigmund [24] which resulted in a non-discrete solution for continuous design variables via a specified elasticity sensor, an artificial density and a penalization exponential. More recently, homogenization approaches dominated by the SIMP approach for topology optimization due to ease of the application. The SIMP model can give the utmost results for the minimum compliance problems and the simplicity of the model greatly provide convenience implementation of topology design in commercial finite element codes [2]. However, the homogenization techniques not only for the elasticity problems. The homogenization techniques preserve its prominent role for multiple physics that are involved by the problem statement. Especially, homogenization of the composite media is crucial for topology optimization of thermal-elastic and electromagnetic based solutions. For instance, an extreme thermally expandable microstructure designed via the topology algorithm proposed by

Sigmund &Torquato, based on interpolation of thermal strain tensor which does not depend on the total density [30].

Hitherto, the mentioned topology optimization methods underscored for elasticity, thermal-elastic problems and etc. propose the globally optimum design if the convex problems are well-posed. Although, the current topology optimization literature provides global solutions of static and thermal stiffness which can be employed for machine tool designs, dynamic behavior prediction and its optimization is also required at early designed stage of machine tool structures. Unfortunately, aforementioned optimization methods cannot depicts envision of dynamic behavior. However, there are also heuristic topology optimization methodologies which are capable of solving a wide range of structural design problems including stiffness, frequency and stress optimization and so on, for locally optimum solutions. Starting with the landmark paper of Xie & Stephen (1993), the first heuristic topology optimization algorithm -which's basic premise is to systematically remove material that appears as the least important to the structure- known as Evolutionary Structural Optimization introduced to the literature [31].The latter studies revealed some problems addressed to the EVO method such as mesh-dependency, checkerboard pattern, and convergence of solutions. Thus, to defeat these displeasing sub-results, Bi-directional Evolutionary Structural Optimization (BESO) method developed which also costs computationally less compered to ESO [32]. Later on, dozens of researches conducted, a lot of developed and augmented approaches proposed such as soft-killed BESO and so on [26].

Today, structural optimization advances are well established, in addition to developments, designs obtained by using topology optimization methods are in production on a daily basis for the industry thanks to various software programs. In 1989, a Japan company released Optishape as the first commercial topology optimization software by using the approach of Bendsoe & Kikuchi (1988). After one year, Optistruct was introduced to the market by former graduates in Michigan (USA). Since then, a lot of CAE-software took places in the market such as, Genesis, MSC/Nastran, Ansys, and Tosca etc. To the knowledge of the reader, all software mentioned above implemented the SIMP method, except Tosca, it used an ESO type

16

method. Recent publications implies also Tosca has started to implement the SIMP approach combined with MMA [33].CAE-software companies have developed similar packages for applications for the aerospace companies such as Airbus, Boeing, NASA and automotive industry such as FORD etc. Unfortunately, this condition is not relevant or secondary affair for the blockbuster machine tool manufacturers although, numerous benefits of lightweight design.

1.2. Research Gap in the Field

As mentioned before, most of the landmark machine tool producers do not employ topology optimization at really early design stage, or it is applied to critical parts even if it is used. Moreover, there is no any dedicated optimization algorithm or any commercial software that is specific to the machine tool design in the current literature and in the market. Therefore, the potential is really high for new studies but, obstacles to be confronted can be listed as the following;

-The ultimate challenge is enormous number of design variables for machine-tool structures even tough stiffness requirements outshine as the objective. The use of mathematical programming methods is a really complicated technique and hard to determine all the design variables simultaneously. Therefore, everything is oversimplified during the beginning of the design phase.

-As stated before, static and thermal displacements and dynamic behavior of the entire structure can be taken as a subset of these stiffness considerations at early design stage. Even though, stiffness, which is expressed in bi-lateral energy form, is consistent with minimization of static, thermal deformations and maximization of eigenvalues. Coupled optimization statements and algorithms that includes consistency of the given energy form, have yet to be discovered [2]

-The conflicting objectives ,such as minimizing the total weight and static torsional and bending compliance, requires a well-balanced trade-off but the establishment of this trade-off is really hard to predict during the beginning of the design due to variety of the component configurations for a machine tool assembly types.

- Another important issue is to simulate realistic virtual models at FE environment for the proper boundary conditions of topology optimization. This attempts come up with

computational problems. Hundreds of publications pointed out the importance of linear guides and spindle bearings during the structural design but these elements are ignored or simply represented due to computational limitations [34]. The reason for that, the underlined junctions are reported as the least stiff elements within the entire structure most of the time and underestimating them leads to unrealistic results.

1.3. The Objective of the Thesis

Regarding the mentioned aspects in the section of 'Research Gap in the Field': this thesis is dedicated to the following objectives below,

- To create realistic and proper boundary conditions with low computational cost at full assembly level for topology optimization of machine tool structures by considering linear guides. Thus, a novel method is proposed for linear guide's roller elements representation in the virtual environment.

- To state a general but simple topology optimization problem by considering commercial optimization codes which can be specified for machine tools.

- To compare design proposals that are given by the same stated optimization algorithm for the proposed new method of the roller elements and oversimplified representations of the rollers, in terms of multiple physics (static, dynamic and thermal).

- To measure and demonstrate the effects of unrealistic roller elements representation for topology optimization application by crossing the representations for the proposed structures.

To expose additional mass reduction opportunities by increasing stiffness of linear guides to obtain lightweight machine tool structures.

1.4. Layout of the Thesis

The thesis is organized as follows; The FEA models and topology optimization of machine tool structures are introduced in Chapter 2.In the next section, two different linear guide representations are presented for the entire assembly of the FE models. The spring based model offers a novel configuration which enables simplicity for assembly level applications

with low computational cost. Additionally, the reliability of these FE models are verified with experiments in Chapter 3. In Chapter 4, topology objectives and constraints are stated. The loading conditions are explained for topology optimization, and then the topology optimization results are compared for two different linear guide's representation. Furthermore, linear guides' stiffness is increased and resultant topologies are demonstrated in Chapter 4.Then, the multi-physics differences between spring-based and contact-based representation are demonstrated for optimized models and the results are compared with original models in Chapter 5. Reliability of the design proposals are measured by crossing the representations for the proposed structures within Section 5.As the last, conclusions are shared in Section 6.

Chapter 2 FEA MODEL AND TOPOLOGY OPTIMIZATION OF MACHINE TOOL STRUCTURES

2.1. FE Models of Machine Tool Structures

Competitive machining centers in the market must have superior design features. To design a lightweight, fast and precise machining centers, FE simulations and topology optimizations are vital. These methods provide predictions about precision and accuracy limits of the machine tool at early design stages. In order to obtain the best reliable results from topology optimization, the FE models of machine tools and the simulation conditions should be close to real ones. However, complexity of the models and computational limitations drive machine tool designers to made simplifications on the machine tools and analyze them in component level. Therefore, all contact surfaces are neglected or underestimated at most of the cases, while machine assemblies' structural behavior depends on the weakest components which are usually reported as linear guides and bearings [3, 4].Thus, to be able to overcome the mentioned computational limits and complexity obstacles, FE-compatible methodologies, which are dedicated to machine tool structures, are developed by researches. The most known ones are listed as the following,

-A. Ertürk et al developed an analytic model by employing Timoshenko beams for spindle-holder-tool assemblies which uses receptance coupling theory .Additionally, they proved that , FRF of the entire structure- as a result chatter and process stability-affected remarkably by

translational bearing and interface stiffness, whereas rotational stiffness of bearings and interface elements contributes slightly [4].

-Another important study is done by Cao and Altıntaş, they offer a semi-analytic method by adding centrifugal force and gyroscopic effects for spindle sub-assemblies [35].

Both of the mentioned FE-compatible methods include sub-assemblies, thus they have to be implemented to rest of the assemblies during FE applications. Therefore, a few new coupled techniques are offered for the entire structure analysis with less computation,

- Co-FEM methods like Multi Body Simulation techniques are coupled with topology optimization to decrease the computational cost. They only modelled the target components as flexible whereas the other components kept as rigid [14]. The biggest problem is here to be able to simulate the entire system behavior after optimization is executed.

- CMS and Model Order Reduction techniques are applied together for machining centers by Law et al [7, 13] by considering the contact interfaces of the main components, but the problem about this solution is underestimating linear guides contact stiffness. Thus, optimization results did not give remarkable results.

To sum up, FE models are required during the construction of design concept to predict static, dynamic and thermal behaviors at early design stage, but their simulation is complex and computational effort is too much. The computationally economic methods, unfortunately not effective for topology optimization, which should be the next stage for the new design proposal. The major reason for that is underestimation of bearing and linear surface contact parameters. Especially, linear surface contact parameters are important for moving components of the entire structure except spindle sub-assembly (for spindle sub-assembly both of them significant). In this study, our focus is structural design of moving components of a five-axis CNC. Thus, realistic representation of the linear guide elements is the key to produce virtual porotypes which are close to real structure. Therefore, linear guide representation techniques are introduced special to machining centers in the sub-section 1 and then, the subjected machining center of the thesis, which is a five-axis milling machine , is introduced and its FE model is given in sub-section 2.

2.1.1. FE Models of Linear Guides Special to Machining Centers

Machining system evolution with different configuration possibilities is a complex processes in the design phase therefore, evaluation and optimization of the final design proposal is derived from Finite Element Analysis (FEA) and Multibody Simulation (MBS) techniques [5, 14].However, Finite element (FE) simulations of machine tools cannot be done directly by using the standard rolling components during the structural design phase due to two reasons:

-The standard rolling elements is not in direct interest during the structural design phase, however linear guides are vital during the design of structural parts.

-The detailed simulation of standard rolling components require huge amount of degrees of freedom (DOF) and computational effort. Therefore, most of the machine tool builders are prone to underestimate these standard elements during the virtual prototyping.

Thus, equivalent linear guide models are necessary for machine tools. In the current literature, two methods are employed special to linear guides for virtual prototyping.

The first is using equivalent contact models directly from FE software library. The utmost problem with this approach is problem formulation and its solution algorithm inside the software. The standard FE contact models confine with node to node or node to surface approach. One element stated as slave whereas the other stated as master and, all of these notions comes from Signorini's contact problem formulation which is presented in 1953 [36].This theory rigorously states the equilibrium problem of a linearly elastic body in contact with a rigid frictionless foundation .As the first solution methodology of this problem, energy functionals used by Fichera [36]. Afterwards, problem and its solution is extended for elastic body with elastic contact. However, the finite element method implementation of the solution is made by Kikuchi [36]for the Signorini's problem [36] and during the rotation; the roller element accepted as a punch type rigid together with an elastic foundation, the identification diameter is considered between them to simplify the complex nature of the problem [36].Therefore, most of the embedded FE contact models uses the-Kikuchi-method-based-algorithms derived for the roller elements assumed as rigid body during the simulation, especially during the rollers rotation solution [36]. This simulation assumptions are vitally crucial during the machine tool structural design. These assumptions directly manipulates the

early stage predictions due to underestimation of rolling elements stiffness especially, when they are evaluated as the least stiff elements of the entire machine tool structure.
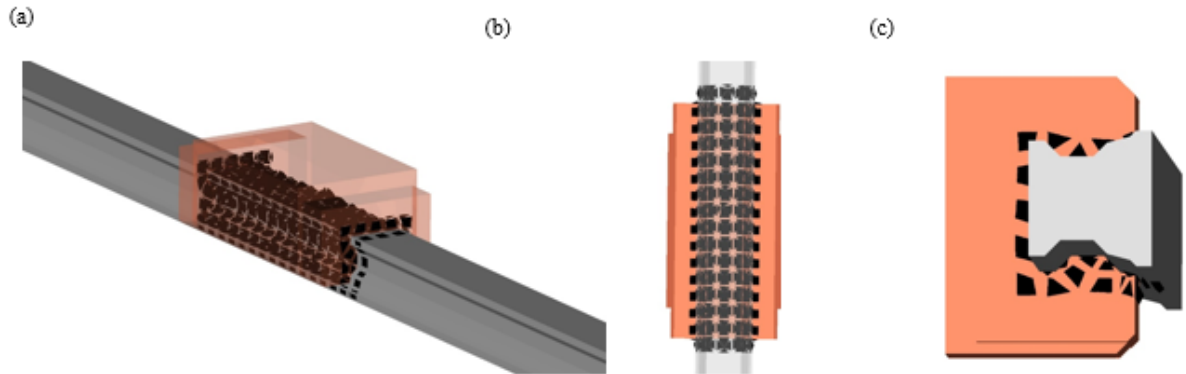
Fig. 1 Contact model from a FE commercial library (a) isometric-view (b) bottom-view (c) side-view

As the second approach, spring-damper equivalent models with translational and/or rotational DOF are employed for standard rolling components of machine tools [3].As the most employed spring-damper system example, rigid or flexible MPC (Multi-Point Constraint) formulation can be given. The manufacturer stiffness directly can be used within the implementation phase of this model. On the other hand, the disadvantage of this method is the unpredicted correlation between stiffness data and geometry. Hence, other methods are developed to get better results such as RIBEM, RoCS and etc by Verl et al [39].To elaborate the given examples, the RIBEM model (Rigid Balls with Equivalent Material) is composed of a rigid roller ball and equivalent material which demonstrates elastic characteristics of roller material and its foundation, but it requires a special calculation method for stiffness. Even though, it requires less computational cost compared to full order models, it is still hard to implement for the entire machine tool structure. Additionally, it depends on the mesh quality at the vicinity of the contact points. Thus a pretension and non-linear spring element replaced with rigid ball with presentation of RoCS (Rolling Contact Spring) model, but the problem is parametrizing concave and a convex body in the equivalent springs. In addition, the error percentage of the model more than 20% due to over-simplification [39].
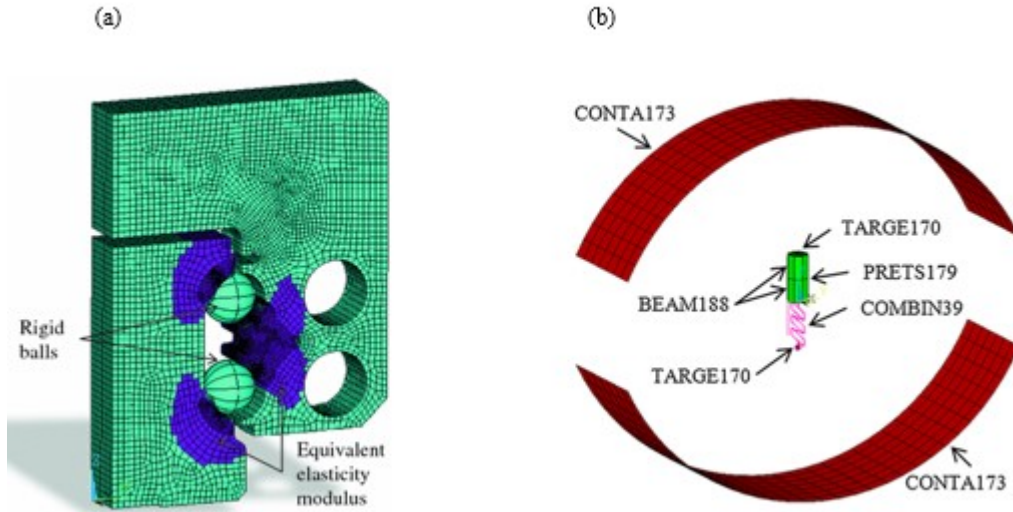
Fig. 2 Spring-damper equivalent models (a) RIBEM model (b) RoCS model [3]

To sum up, the mentioned virtual models of machine tools' linear guides have significant sides and also drawbacks. However, they still need development for implementation of the entire machine tools structures with a realistic approach and with a low computational cost. The significant effect of this development will be seen multiple physics predictions of the machine tools during early design stage .Because boundary conditions directly affects design proposals of the topology optimization and linear guides can be stated as boundary areas for multi-component level optimizations. Thus, a novel linear guide presentation is proposed within section 3.2.

2.1.2. FE Model of the Subjected Five-axis Milling Machine

The subjected machining center for this thesis is Spinner U1520 which is a five-axis CNC. The subjected CNC is presented visually in Fig. 3a and its CAD representation without out shells is demonstrated in Fig. 3b.
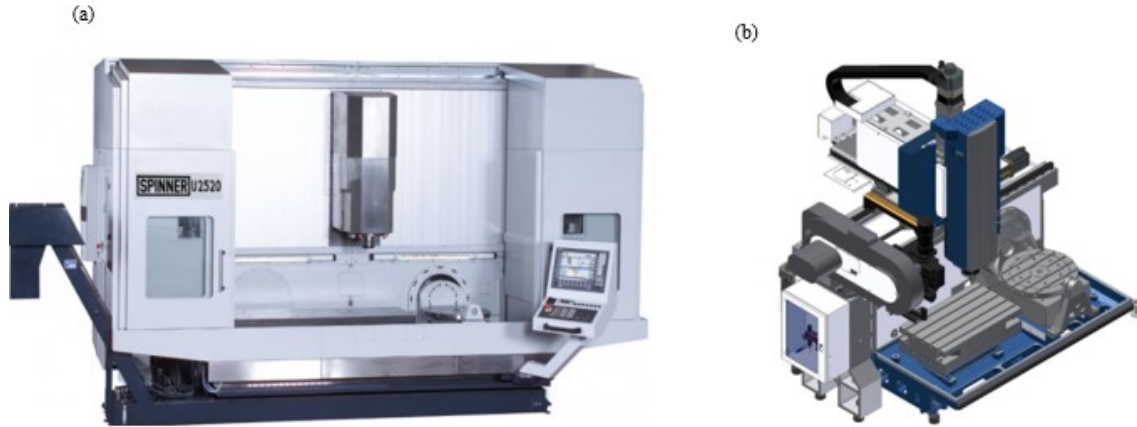
Fig. 3 Spinner U 1520 (a) Real model (b) CAD model without outer shells [37]

The five-axis milling machine FE models are generated by using its respective CAD models via Hypermesh. Each structural component of the model is meshed with tetra elements, with total of ~ $4\text{x}10^6$ elements and ~$1\text{x}10^6$ nodes, after a convergence test. Three material properties, for steel and cast iron assigned to different components of the model are given in Table 1.

Table 1Material properties assigned to components

Material	Elasticity Modulus	Density	Poisson Ratio
Steel	210 GPa	7850 kg/m^3	0.3
Cast Iron	140 GPa	7200 kg/ m^3	0.3

The FE model is created for the full-assembly level of structural components. The chip conveyor and automatic tool change system is excluded from the FE models, and the servo-drives are represented as point masses by employing point load mass and RBE3 elements. In addition worktables, are represented with distributed loads. For static and   thermal simulations, Optistruct is used whereas Radioss is employed for dynamic analyses. The respective FE model is depicted in Fig.4 as meshed version.

25
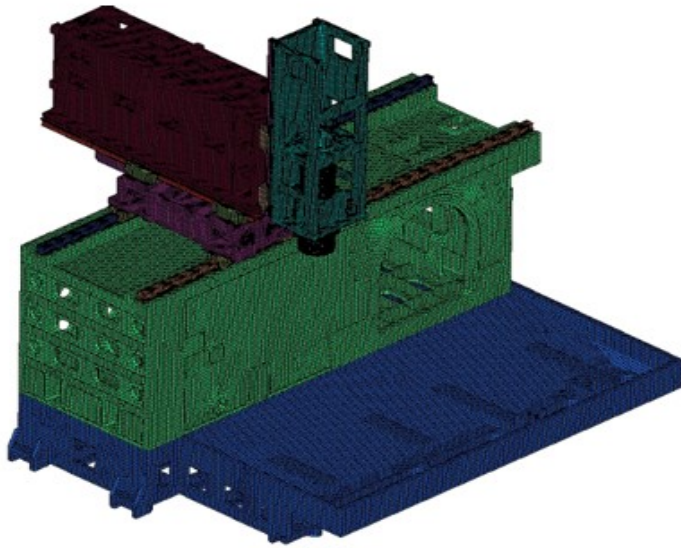
Fig. 4 FE model of Spinner U 1520-meshed version

As mentioned before, linear guides are the vital key to obtain realistic FE models. Thus, the employed linear guide types are introduced in this section. Three different types of Bosch-Rexroth linear guides are used within the assembly. The first is SLH 35 type which is located between the spindle head and the ram. The second is SLH 45 type and it is located between the ram and the sliding carriage. The third is FLS and located between the sliding carriage and the main frame. Moreover, roller type rolling elements are assembled for all this C3 (13% preload)   type preloaded models [38]. These models are separated from each other with their runner block types and they are named according to runner block types. The raceway is same for both FLS and SLH runner blocks. The used runner models and raceways are demonstrated in Fig. 5.
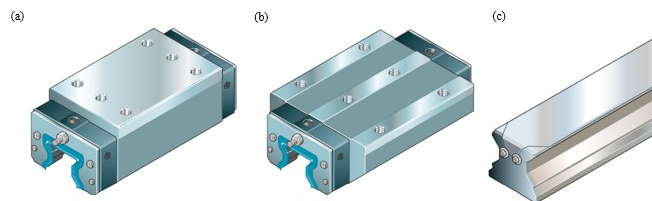
Fig. 5 Bosch-Rexroth linear guide components (a) SLH type runner (b) FLS type runner (c) raceway [38]

As stated previously, equivalent models are required for linear guide FE representations .In the current literature two methods employed special to linear guides for virtual prototyping the first one is contact modelling whereas the second is spring modelling for the roller elements of linear guides. In this study, FE models are constituted for the both of the methods. The details will be elaborated in Section 3. The two employed models are illustrated in Fig. 6, the contact-based is named as Model 1 whereas the Model 2 is established for spring-based approach.
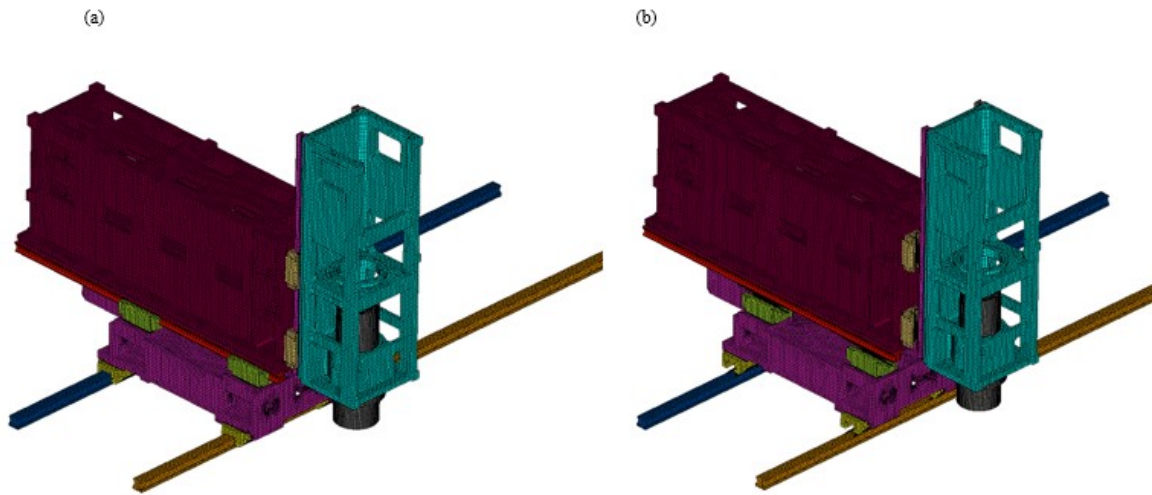
Fig. 6 FE model of moving components (a) Model 1 (b) Model 2

2.2. Topology Optimization of Machine Tool Structures

Topology optimization should be a primary optimization technique after FE analysis are completed for a new CNC concept. The reason for that, material can be redistributed without any initial design requirement for the selected objective by employing topology optimization, and then shape and sizing optimization can be employed to finish of the design stage. The problem statement and objectives are vital during the topology optimization stage, because the solution technique is determined according to objective. Thus, solution technique defines global or local optimum for the proposed optimization. The initial design objectives can be listed as the following, which are special to lightweight machine tool structures;

-Maximum stiffness (Minimum compliance)

-Maximum frequency

-Minimum stress distribution

- Minimum thermal displacement

 It is noteworthy to remind that during the solution stage of single-objective optimization problems, the maximum stiffness and minimum thermal displacement objectives can be solved globally, by employing micro-structure techniques, while maximum natural frequency and minimum stress objectives can be solved locally in general by employing macro-structures techniques.

On the other hand, statement of all objectives as multi-objective design optimization problem is really complicated. Additionally to combine them by using micro-structure techniques is not seen possible. Because the specific proves of maximum frequency problem by employing micro-structures techniques have yet to be explored for a global solution. Another obstacle to combine all of the objectives is about stress-based topology optimizations. Due to stress singularity, reaching a global optimum for a stress-based topology optimization is not guaranteed during the computational process, therefore it is applied locally. There is no specific methodology or problem formulation dedicated for machining centers in the current literature due to the mentioned difficulties.

However, it can be applied step by step for single-objective problems, beginning form the minimum compliance problem. Because structural stiffness defines precision and accuracy of the machine tools, also it is guaranteed the global optimum since the problem is well-posed. The most common topology optimization formulation is developed to obtain stiffer structure by minimizing the compliance subject to a given amount of material, [2]. Basically, minimizing compliance equals to minimizing the energy of deformation at the equilibrium state of the structure. This problem in a continuous form can be stated as the following;

$$min_{\rho} : \varphi(\rho) = \boldsymbol{F}^T \boldsymbol{U} \tag{1}$$

$$s.t. : \sum_{e=1}^{N} v_e \rho_e = \boldsymbol{v}^T \boldsymbol{\rho} \leq V^*, e = 1, \dots, N \tag{2}$$

$$: g_i(\rho) \leq g_i^*, \quad i = 1, \dots, M \tag{3}$$

$$: 0 \leq \rho_{min} \leq \rho \leq 1 \tag{4}$$

$$: \boldsymbol{K}(\boldsymbol{\rho})\boldsymbol{U} = \boldsymbol{F} \tag{5}$$

Within a given domain (Ω) by discretizing N finite elements. Here, the density depends on compliance as $\varphi(\rho)$ objective function with a volume constraint V^*, where, $\boldsymbol{F}, \boldsymbol{K}$ and $\boldsymbol{U}$ stand for force vector, global stiffness matrix, and nodal displacement vector, respectively. The displacements of the components are limited with a displacement constraint, which is represented by g_i^* in the problem statement.

For this problem formulation, boundary conditions are not the major interest since it is executed in component level for critical machine tool parts. However, boundary conditions affect the problem solution if the design domain covers the entire assembly or most of the components. Because, linear guide areas and its vicinity resemble boundary conditions for a milling machine, thus the multi-physical behavior transmission is crucial to obtain true design proposals from the employed topology optimization algorithm. Another important side is about boundary conditions: if they can be constrained as real, it is possible to maximize the expectation of 'maximum dynamic compliance' and 'min thermo-elastic displacement' due to 'minimization of compliance' for topology optimization applications. Because, as mentioned before, minimum compliance problem is stated according to bi-lateral energy form of a continuum structure. Thus, the minimum compliance problem is executed to show significance of the proper boundary conditions for topology optimization of the entire CNC structure. Realistic and unrealistic boundary conditions are compared within this thesis. Optistruct solvers are used to solve the stated topology optimization problem. In the next section, linear guides contact modelling will be presented to resemble realistic and unrealistic boundary conditions.

Chapter 3 **LINEAR CONTACT MODELLING**

Nowadays, linear guide components have been in a crucial role for high positioning accuracy for machine tools. It is proved that, machining performance changes according to positions of preloaded linear rolling elements [39] for milling machines. It is also reported that, these elements affect the entire machine structure's stiffness, because most of the cases, they are tagged as weakest components of assemblies in the literature [3, 4].Thus, their realistic representation is vital for the FE model and the topology optimization phase of the entire assembly, but as mentioned before, linear guides' roller elements are oversimplified or underestimated due to computational issues. To be able to demonstrate effect of roller elements during the topology optimization stage, two virtual linear guide models are introduced in Chapter 3.1 and Chapter 3.2 (Model 1&2).

3.1. Contact Representation for Linear Guides (Model 1)

As mentioned previously, in Section 2.1.1 Signori's contact model was solved for FE implementations by Kikuchi for the original problem statement. Most of the FE commercials used Kikuchi-based-solution for the contact models embedded their library. Thus, roller elements accepted as rigid to simplify solution which leads the unrealistic representation for linear guide elements. In this section embedded contacts are used from Optistruct library to resemble the linear guides' roller elements. The employed contacts are illustrated in Fig.7
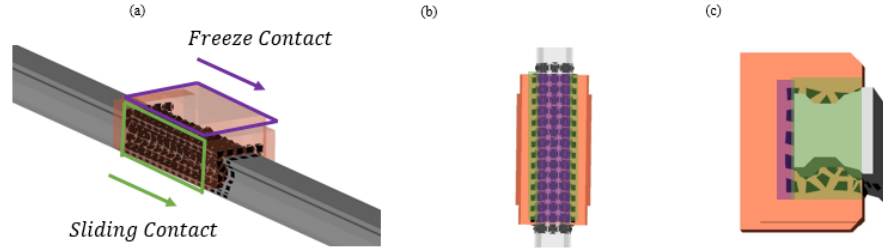
Fig. 7 Contact model from Optistruct library (a) isometric-view (b) bottom-view (c) side-view

As it can be seen from the Fig.7, sliding contacts are plugged in the assembly through the movement axis of linear guides, while freeze contacts are employed for the other axis directions. These contacts only employed for translational directions, because rotational axis have minor effect on structural stiffness which is proved before by Ertürk et al [4].

3.2. A Novel 3-D Representation for Linear Guides by Using 1-D Springs (Model 2)

3.2.1. FE Configuration of the Proposed Linear Guide Representation

In this study, our aim is to demonstrate a novel and easy FEM approach to represent rolling elements of linear guides. In the current literature, full order models, rigid representations and spring models are available for rolling elements by employing co-FEM, MBS and pure FEM methodologies. Full order models are computationally costly and rigid models have consistency problems between MBS and FEM software. Therefore, its implementation is not an easy task. On the contrary, springs offer easier and realistic representation solutions.

In our study, rolling elements are modelled via 1-D springs to represent rollers' 3-D behaviors. Spring elements are employed between guide rail and runner block. According to our configuration, two cross-settled rollers are represented by one spring element. It is noteworthy to state that, settlement of these springs are at transversal direction for the entire linear guide representation. The reason for transversal settlement is to carry loads in two directions. The third direction is free movement direction of linear guides. Therefore, linear

guide's real behavior imitation is possible for three direction in terms of static and dynamic stiffness. The mentioned configuration is presented visually in Fig 8.
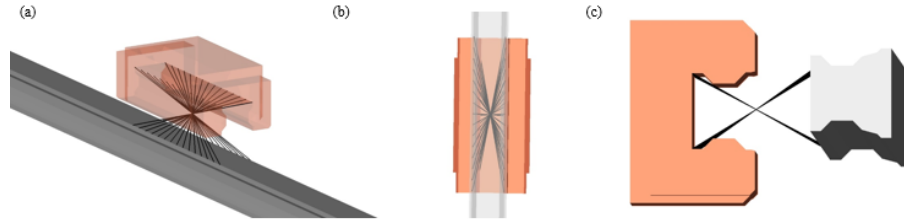
Fig. 8 Transversal springs for roller elements (a) isometric-view (b) bottom-view (c) side-view

The other spring configurations are taken from the available literature, and presented at here to give a rough idea. The first group of spring representation works for each direction. However, compared to our configuration, error percentages are higher. The second spring representation offers more realistic results but it is not easy to implement.
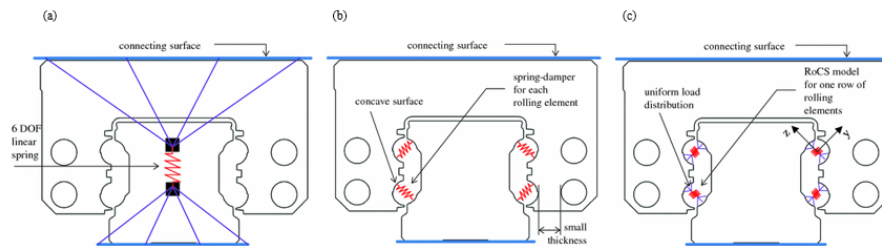
Fig. 9 Spring representations for roller elements (a) MPC model (b) Classic model (c) RoCS model [39]

3.2.2. Semi-Analytic Stiffness Calculation for Rolling Elements

In the model, our aim is embedding 'contact stiffness values' to the 1-D transversal springs in order to simulate realistic behavior at early design stage. Hertzian contact theory can be an analytical option to calculate contact stiffness between a smooth sphere / cylinder and a smooth flat / cylindrical foundation. However, the problems with analytical Hertzian approach can be counted as follows;

- Results must be evaluated according to machining surface roughness,
- Asperity heights affect the behavior to be seen, therefore a Gaussian distribution is required at microscale level [40].
- Lubricant and wear debris effects are ignored.

Thus, semi-analytic methods, which contain average amounts of surface roughness, asperity and lubricant effects, should be employed. In the current literature, an ERA-based test method is proposed by Shi et al [41]. Basically, ERA is a time-domain realization technique which uses least-squares method by using a singular value decomposition to detect the model order. The 'Eigen system Realization Analysis' method requires a special test setup. Therefore, it is still far away from being practical for a machine tool designer. Also, Shi reported that, ERA and Hertz theory give nearly same results for small range displacements [41]. Hence, a semi-analytic method is proposed, which is based on Hertzian contact and liner guide manufacturer deflection experiments.

As mentioned earlier, Spinner U1520 is the subjected five-axis CNC for this thesis. Three different types of Bosch-Rexroth linear guides are assembled to the five-axis CNC. The first is SLH 35 type which is located between the spindle head and the ram. The second is SLH 45 type and it is located between the ram and the sliding carriage. The third is FLS and located between the sliding carriage and the main frame. Moreover, roller type rolling elements are assembled for all this C3 type preloaded models. Therefore, linear elastic contact is observed for cylinders and flat foundations.
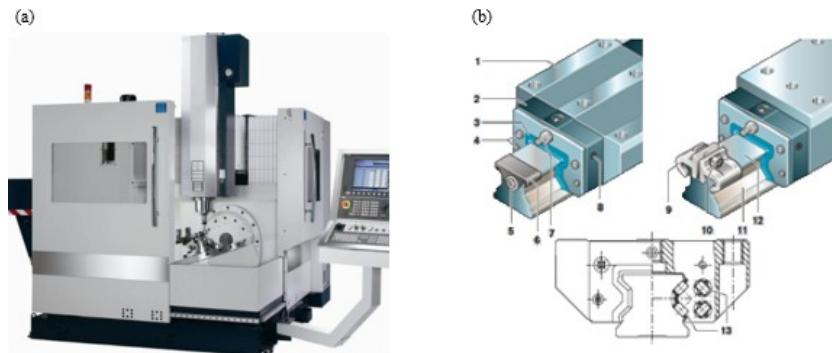
Fig. 10 (a) Spinner U1520 Five-axis CNC [37] (b) Bosch-Rexroth Linear Guide [38]

33

Experiment data can be obtain from manufacturer catalogues in the forms of down loading, lift-off loading and side loading .The deflection data occurs here due to line contact, because the roller shape is cylinder. Albayrak [16] proved before, the Hertzian line contact calculation is consistent with experiment data of the manufacturer. Therefore in order to calculate stiffness data, experimental deflection data is used directly. The manufacturer's loading conditions are illustrated in Fig 11.
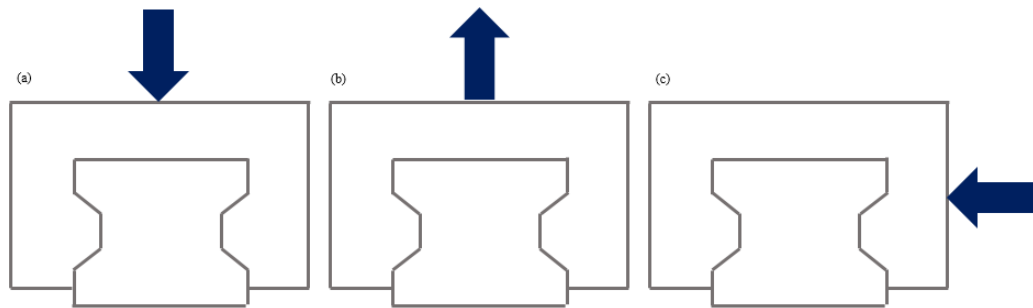
Fig. 11 The manufacturer loading configurations (a) down loading (b) lift-off loading (c) side loading

Stiffness calculation is based on usage of experiment data and Hertz Line Contact. Therefore, after finding the force amount per roller, normal force and normal deflection should be calculated for one roller. In order to calculate stiffness of the first translational axis, average of down-load and lift-load stiffness should be derived from Hertz theory by using experimental deflections. Side-load stiffness should be found to complete calculation of the stiffness of the second translational axis. The third translational axis is the linear guide's movement axis, thus it is not considered.
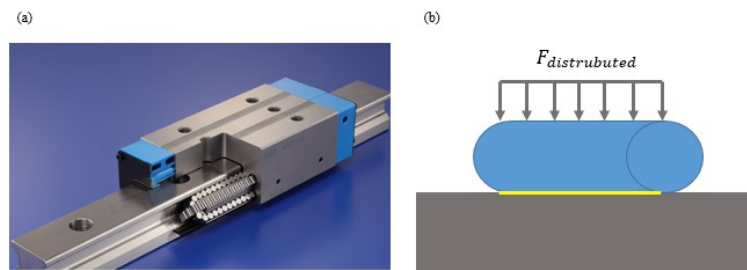
Fig. 12 (a) Sectional view of a roller type linear guide [38] (b) Hertezian Linear Contact

In order to begin the stiffness calculation process, the inspection scope should be narrowed from the load amount carried by one linear guide to per roller. Force values of per roller are given by Equation (6),

$$F_R = \frac{\sum F_{exp}}{\sum R} \tag{6}$$

Where F_{exp} is total force whereas R is the roller number for a linear guide. Afterwards, normal force of per roller should be calculated. The normal contact force depends on the geometrical design and can be stated by Equation (7).

$$Q = \frac{F_R}{\sin \beta} \tag{7}$$

As the next step, deflection data should be read from the manufacturer catalogues for the selected F_{exp} value. Then, normal deflection should be derived from the manufacturer data again considering geometrical features (β) and its relation with experiment data can be stated by Equation (8).

$$\delta_N = \delta_{exp} \times \sin \beta \tag{8}$$

Where δ_{exp} is experimental deflection data while δ_N is its normal resultant. After calculation of normal deflection, stiffness should be calculated for one roller by help of Hertz contact theory. Q denotes the contact force and δ_N is the elastic deformation at the contact point. K_h represents the Hertz constant, which is determined by the contact geometry and material properties of the linear components and it can be given by Equation (9).

$$K_h = \frac{Q}{\delta_N^{3/2}} \tag{9}$$

Finding roller's normal stiffness is the next step for the subjected experiment conditions. Stiffness formulation is expressed via Equation (10) by help of Hertzian contact theory.

$$K_n = \frac{3}{2} \times K_h \times \delta_N^{1/2} \tag{10}$$

As the last, 1-D spring stiffness can be found by rate and ratio calculations by considering number of springs in the FE model. S denotes the number of the 1-D springs employed in the FE model for one linear guide.

$$K_{FE\_spring} = \frac{K_n \times R}{S} \tag{11}$$

The average of down-load's and lift-load's K_{FE_spring} can be used as the stiffness value of the first translational axis, whereas half of the side –load's K_{FE_spring} can be taken as the stiffness value of second translational axis due to geometric features.

A calculation example is presented here for 5000 N. The deflection data is tabulated in Table 2 according to manufacturer experiment data [38].

Table 2 Manufacturer Deflection Data for 5000 N loading

Linear Guide Type	SLH35 Deflection	SLH45 Deflection	FLS45 Deflection
Down loading	2.75 μm	1.29 μm	1.96 μm
Lift-off loading	3.77 μm	1.44 μm	2.49 μm
Side Loading	7.14 μm	4.11 μm	2.67 μm

The contact stiffness calculation results for down, lift-off and side loads are presented in Table 3.

Table 3 Stiffness Calculation in case of 5000 N loading

Variables		SLH35 Down	SLH35 Lift	SLH35 Side	SLH45 Down	SLH45 Lift	SLH45 Side	FLS45 Down	FLS45 Lift	FLS45 Side
F	(N)	5000	5000	5000	5000	5000	5000	5000	5000	5000
F_R	(N)	73.53	73.53	147.06	59.52	59.52	119.05	59.52	59.52	119.05
Q	(N)	51.99	51.99	103.99	42.09	42.09	84.18	42.09	42.09	84.18
δ_{exp}	(µm)	2.75	3.77	7.14	1.29	1.44	4.11	1.96	2.49	2.67
δ_N	(mm)	0.0039	0.0053	0.0101	0.0018	0.0020	0.0058	0.0028	0.0035	0.0038
K_h		214375	133822	102419	537030	456329	190172	287755	201421	36279
K_{FE_roller} (N/mm)		20053	14647	15441	34473	30927	21740	22742	17929	33440
K_{FE_spring} (N/mm)		45455	33201	17500	103420	92780	32610	53065	41834	39014

According to results for the first linear guide type, one of normal translational contact stiffness is calculated as ~20 KN/mm, the second which refers tangential translational contact stiffness is predicted as ~17 KN/mm. For the second linear guide type, normal and tangential contact stiffness of the springs are computed as ~49 KN/mm and ~32 KN/mm respectively while these values are reported as ~23 KN/mm and ~39 KN/mm for the third linear guide type. The results are verified with the static and dynamic experiments later on.

3.2.3. Reliability of the Proposed Linear Guide Representation

In this part, the proposed linear guide model is compared with equivalent contact models which is embedded in FE software library. The mentioned linear guides are named as Model 1&2 for better understanding. Roller elements are modelled as surface contacts for Model 1 by using FE library, while the proposed linear guide method is employed for Model 2.
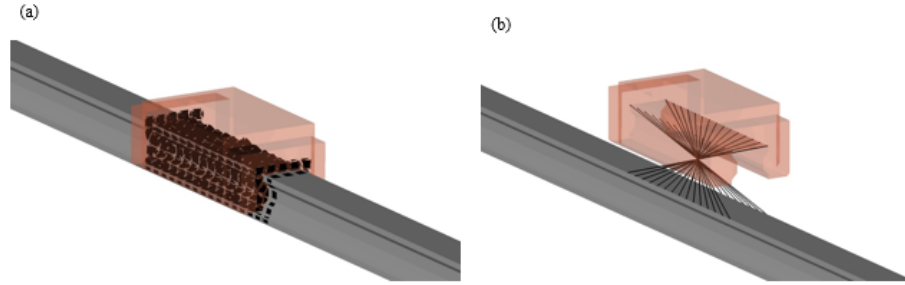
Fig. 13 (a) Model 1 surface contacts for rollers elements, (b) Model 2 springs for roller elements

3.2.3.1. Static Reliability Experiments

In order to understand directional stiffness behavior of the full assembly, the spindle tip is loaded in various directions in real and virtual environment. Verification experiments are conducted [16] to measure the static deformation of the machine tool spindle in five different positions.
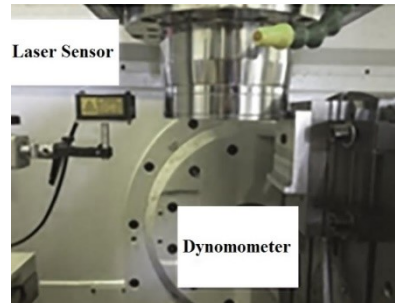
Fig. 14 Experimental set-up for static experiments

The machine tool spindle tip is loaded in X direction of the machine during the first three experiments while it is loaded in the machine's Z direction during the fourth and the fifth experiments. Both experimental and FE results are tabulated in Table 4 and Table 5 for equivalent contact Model 1 and 2, respectively.

Table 4 Equivalent contact Model 1 surface contact for rolling elements

Experiment Number	Applied Force	Experiment Result	Analysis Result	Difference
1	520N	20 μm	8.4 μm	58%
2	455N	20 μm	8.3 μm	59%
3	375N	24 μm	10 μm	58%
4	485N	13 μm	3.7 μm	71%
5	265N	6.5 μm	1.5 μm	77%

Table 5 Equivalent contact Model 2 spring for rolling elements

Experiment Number	Applied Force	Experiment Result	Analysis Result	Difference
1	520N	20 μm	21.3 μm	7%
2	455N	20 μm	19.5 μm	2%
3	375N	24 μm	23 μm	4%
4	485N	13 μm	11.9 μm	8%
5	265N	6.5 μm	6.7 μm	3%

The comparison of the experimental and FE results for both models indicate significant discrepancy which is caused by representation of the rolling elements. Although the first equivalent model has its own stiffness value, the rolling elements are underestimated. Instead of these underestimated rolling elements, built-in contact elements are employed which is computationally less expensive. However, these substitutes are not performed enough. This performance evaluation could be observed obviously in Table 4. On the contrary, the second

equivalent model is employed springs to directly represent rolling elements even though this method is computationally costly. Although this cost, the return is significant as indicated in Table 5.

3.2.3.1. Dynamic Verification Experiments

In order to understand dynamic reliability of the proposed method (Model 2), it is subjected to a dynamic experiment virtually. FRF response of the full-order assembly model is simulated. Then, hammer tests are conducted to measure the real FRF response. The experiments are designed to measure FRF responses of the least stiff and most stiff position of the entire assembly. Therefore, the machine tool assembly is positioned at positive/negative limits of Y and Z axis. The measurement is conducted along X-X axis. On one hand, Hammer Test 1 is conducted for the most rigid position of the CNC assembly. Thus, the machine tool is positioned at maximum limits of the Y and Z axis. On the other hand, Hammer Test 2 is conducted for the least rigid position of the CNC assembly. Hence, CNC is positioned at minimum limits of Y and Z axis. Spindle tip is excited for both test conditions, in order to catch structural components' modes. The same positioning procedure is imitated for the FE simulations. Model 2 is employed for the all linear guides, and FE models are simulated for the full-assembly level. The Hammer test positions of the CNC are illustrated below in Fig. 15.
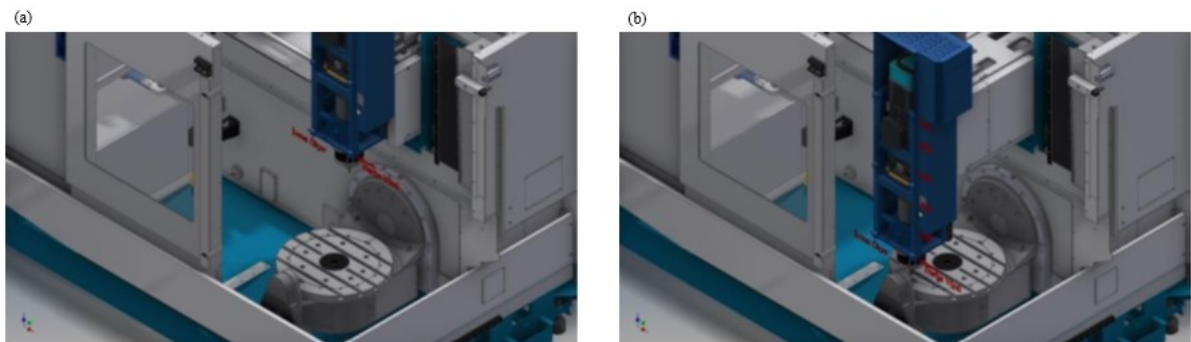
Fig. 15 (a) Hammer Test 1 - refers the most rigid position, (b) Hammer Test 2 - refers the least stiff position of the CNC structure

Experiments' and FE simulations' FRF responses are indicated for the minimum and maximum positions of the CNC assembly in Fig 16. The red lines indicates the least stiff position of the assembly, while the black lines indicates the stiffest position of the assembly. The continuous lines refer experiment results whereas the dashed ones refer the FE simulations for the proposed virtual linear guide representation (Model 2).
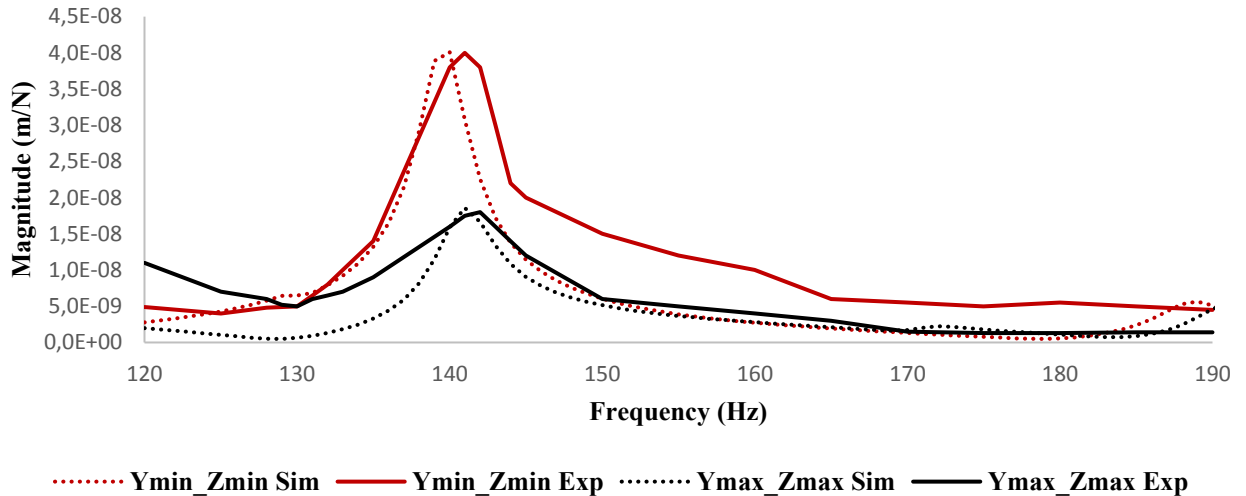
Fig. 16 FRF results for Hammer Test 1&2 and FE simulations

Fig.16 reveals the reliability of the proposed virtual model (Model 2).The dominant mode of the structure is reported as 142 Hz from the experiments for the max and min positions while these modes are simulated as 140 Hz by FE simulations of the full-assembly .In other words, it equals ~1, 4% error for early design stage predictions. Another significant result is about the magnitude values, only 10% material damping is used during the simulations and there were no extra damping data. The FRF magnitudes of FE simulations are also compatible with the dominant FRF magnitudes of experiments. For example, the modal flexibility of the FE simulation is reported as 1, 86E-8 m/N for the dominant mode while it is reported as 1, 8E-08 m/N by experiment results for the stiffest position. This FRF result similarity also can be observed at least stiff position. The gap between simulation and experiment results can be reduced by using proportional damping for the future studies.

As the last word, a new virtual method for linear guide's roller representation (Model 2) is proposed and explained within this section. Its reliability is proved with static and dynamic experiments. Additionally, the reliability of the contact models, which are already embedded in commercial FE software, are examined with static experiments. The superior side of the new proposed model is easy implementation and simple calculation methodology compared the existing virtual models. Moreover, the new model is easily applicable for the entire assembly level simulations with low error percentages and low computational cost. The next chapter will compare differences of the design proposals for the same topology algorithm, when the linear guides virtually represented with the proposed model and surface contact models.

Chapter 4 **EFFECTS OF ACCURATE LINEAR CONTACT REPRESENTATION IN TOPOLOGY OPTIMIZATION OF MACHINING CENTERS**

Topology optimization is a countermeasure to obtain lightweight and stiff structures for machine tools. Topology optimizations are applied at component level due to computational limitations, therefore linear guides' rolling elements are underestimated in most of the cases. Stiffness of the entire assembly depends on the least stiff components which are identified as linear guides in the current literature. In this study, effects of linear guide's representation in virtual environment are investigated at assembly level by focusing on topology optimization. Two different contact models are employed for rolling elements in the linear guides. Reliability of the contact models are verified with previous experiments. After the verification, heavy duty cutting conditions are considered for the system and topology optimization is performed for two different contact models to reduce the mass of the structure. The difference caused by the representation of rolling elements is demonstrated for the same topology algorithm and the optimization results are compared for the models. Lastly, the effect of using more stiff linear guides in the five-axis milling machine is investigated by increasing the stiffness of the contact elements.

4.1. Equivalent Linear Guide Models: Model 1 and Model 2 revisited

In this part, different FE-based representations of a linear guide are revisited to remember which are given in Section 3. These two approaches are employed to resemble contact elements at the assembly level. Reliability of these FE models are verified before with static

tests. Roller elements are modelled as surface contacts in Model 1 while the proposed linear guide method is employed for Model 2. Revisited models are shown in Fig. 17.
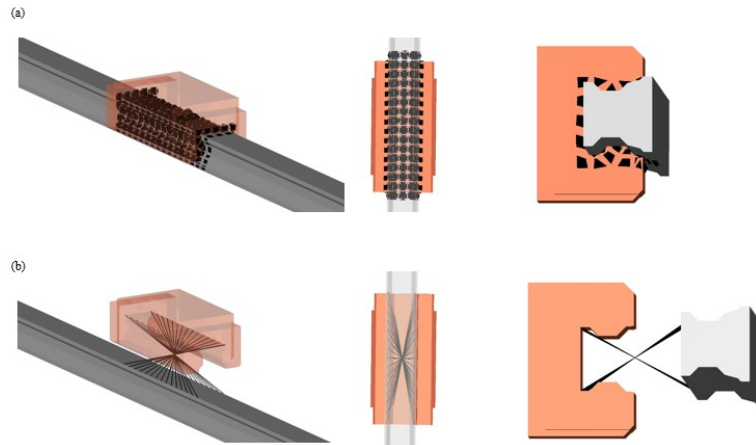
Fig. 17 Revisited virtual linear guide representations (a) Model 1 surface contacts for rollers elements, (b) Model 2 springs for roller

4.2. Loading Conditions for Topology Optimization

For topology optimization, heavy cutting conditions are applied for a tapered helical ball end mill cutter [15], which are commonly used in machining of complex surfaces such as air foils, in the FE simulations. Titanium Ti6Al4V alloy is chosen as the workpiece material. Axial depth of the cut is 20mm and feed rate is 0.050mm/tooth. The cutting forces are obtained via CutPro software for the conditions indicated in [15]. Static and modal analysis are performed by using the resultant cutting loads. FE simulations are repeated for two contact models. Based on the static analyses, total spindle deflection at the spindle tip is determined 22 µm for the first contact model while it is 55 µm for the second model. Additionally, based on modal analysis, the natural frequencies of both models obtained by the finite element solution are illustrated in Fig 18.
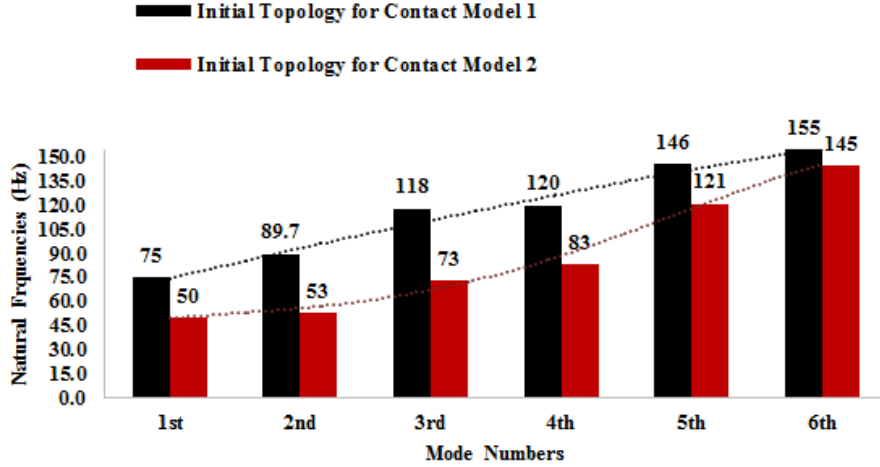
Fig. 18 Natural frequencies of given initial design for the first six modes

As can be seen from Fig.18 the differences are considerable for the first four modes for Model 1 and Model 2. The gap closes dramatically when the fifth and sixth modes are considered. The gap reduces nearly zero for the higher modes, but as mentioned before [1] at low frequencies servo drive and machine structure modes may overlap and cause instability The usual way to overcome this is to reduce gains for the servo drivers which limits the running range of the servos reducing acceleration/deceleration rate. Therefore, in order to reach upper limits of servo drivers and increase speed performance of a machine tool, simulation of the structural models with realistic predictions especially for the low modes, are vital during design stage. Furthermore, pushing the low modes to higher frequencies as much as possible through mass reduction would not only increase the servo performance and acceleration and jerk limits of the machine axes but also reduce energy consumption.

4.3. Topology Optimization Problem Statement

The most common topology optimization formulation is developed to obtain stiffer structure by minimizing the compliance subject to a given amount of material. This problem in a continuous form can be stated as the following;

$$min_\rho : \varphi(\rho) = \boldsymbol{F}^T\boldsymbol{U}$$

$$s.t. : \sum_{e=1}^{N} v_e\rho_e = \boldsymbol{v}^T\boldsymbol{\rho} \leq V^*, e = 1, ..., N$$

$$: g_i(\rho) \leq g_i^*, \quad i = 1, ..., M$$

$$: 0 \leq \ \rho_{min} \ \leq \rho \leq 1$$

$$: \boldsymbol{K}(\boldsymbol{\rho})\boldsymbol{U} = \boldsymbol{F}$$

Within a given domain (Ω) by discretizing N finite elements. Here, the density depends on compliance as $\varphi(\rho)$ objective function with a volume constraint V^*, where, $\boldsymbol{F}, \boldsymbol{K}$ and $\boldsymbol{U}$ stand for force vector, global stiffness matrix, and nodal displacement vector, respectively. The displacements of the components are limited with a displacement constraint, which is represented by g_i^* in the problem statement. The displacements of the components are limited; (1) on the spindle tip, (2) on the maximum deflected areas of the moving components, which are spindle head, ram and sliding carriage.

The optimization results show that the plotted topologies were exactly same for the (1) and the (2) displacement limitations. Therefore, the displacements are limited on the spindle tip during the whole optimization.

For the volume constraint, an iterative volume fraction process is applied to explore mass reduction capacities of the given five-axis milling machine. In the optimization, volume fraction rate is set to 20%, 25% and 30%, respectively. It was seen that higher than 30% volume fraction rate caused violation of displacement constraints.

4.4. Topology Optimization Results

4.4.1. The Optimal Topology for Model 1

The moving components of the initial design are optimized to obtain minimum compliance for the given constraints in the problem statement. The re-designable components are chosen as spindle head, ram and sliding carriage which are the most active parts in the given assembly. As a result of the optimizations, element densities are shown in Fig.19.

Fig. 19 Topology Optimization Results for the Model 1 with volume fraction constraint (a) 20%, (b) 25% and (c) 30%

Blue regions indicate optimum mass reduction areas while red regions illustrate compulsory areas for the stiffened structure. The elements with low density are removed and the resulting structure with 30% volume fraction is shown in Fig 20.
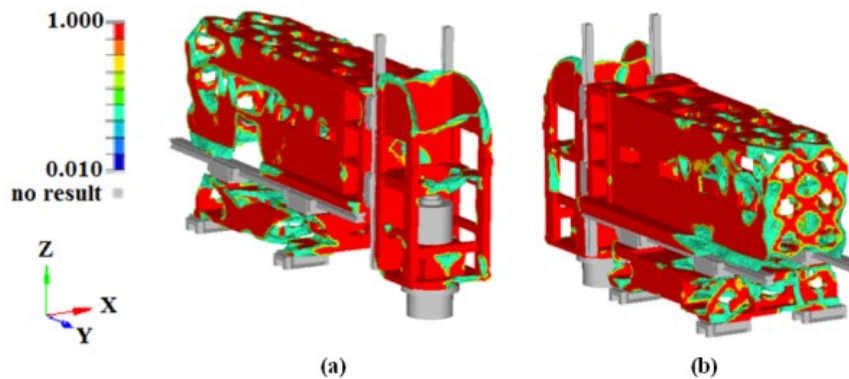
Fig. 20 (a) Front View of Top. Opt. for Model 1, (b) Back View f Top. Opt. for Model 1

4.4.2. The Optimal Topology for Model 2

Same as Model 1, optimization results for Model 2 are given in Fig. 21. Even though, there are ~ 60% difference in static response behavior and around ~40% difference in dynamic response behavior between Model 1 and 2, their optimal topologies are similar. Nevertheless, the optimized topologies of connection areas with linear guides are very different. The reason for that is the higher rigidity of Model 1 due to neglected contact stiffness. The resulting structure with 30% volume fraction is shown in Fig 22.
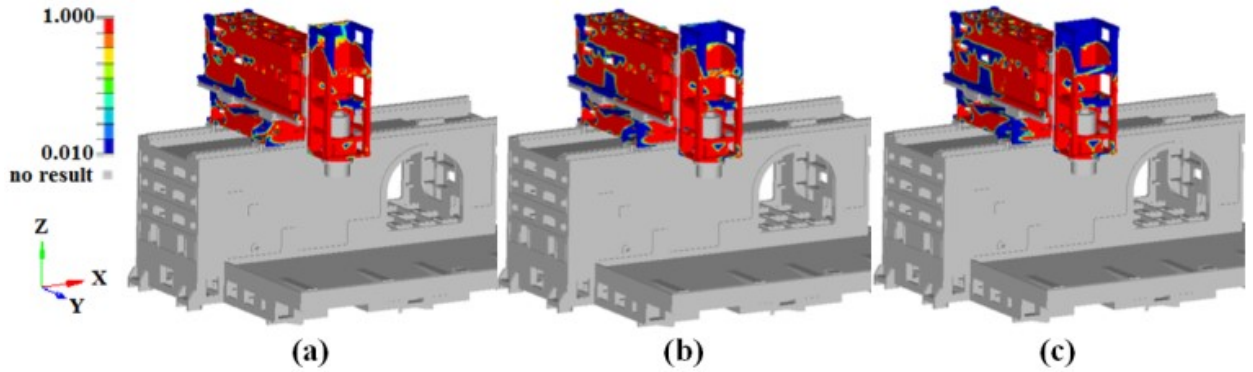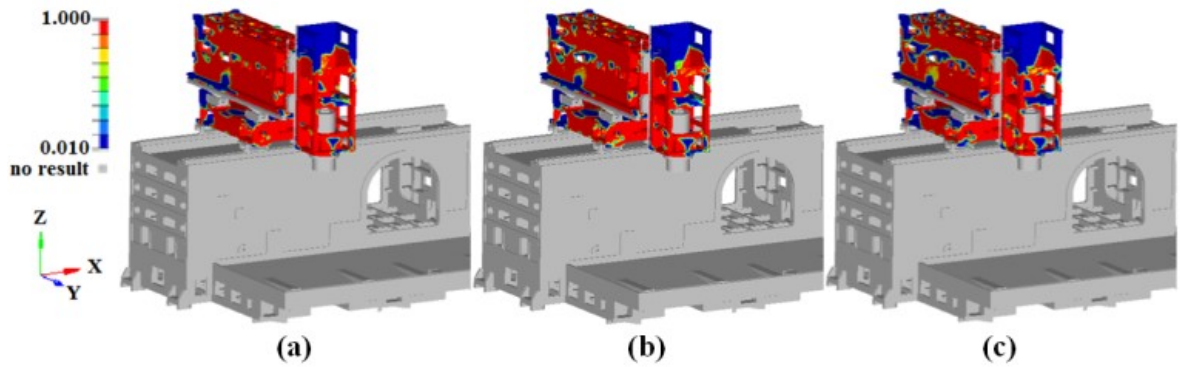
Fig. 21 Topology Optimization Results for the Model 2 with volume fraction constraint (a) 20%, (b) 25% and (c) 30%
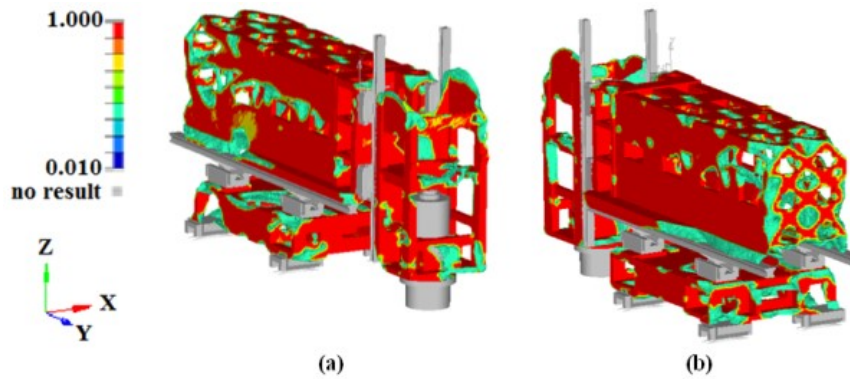
Fig. 22 (a) Front View of Top. Opt. for Model 2, (b) Back View of Top. Opt. for Model 2

4.4.3. Comparisons of the Results for Model 1

Although, there is a remarkable difference between the static and dynamic response behaviors of the models, the resultant optimized topologies are similar. However, difference occurs in the neighborhood of the linear guides. According to topology optimization results, the volume fraction intensity in the neighborhood of linear guides is noticeable for Model 2, while it is the reverse for Model 1. The differences are illustrated clearly in Fig.23.
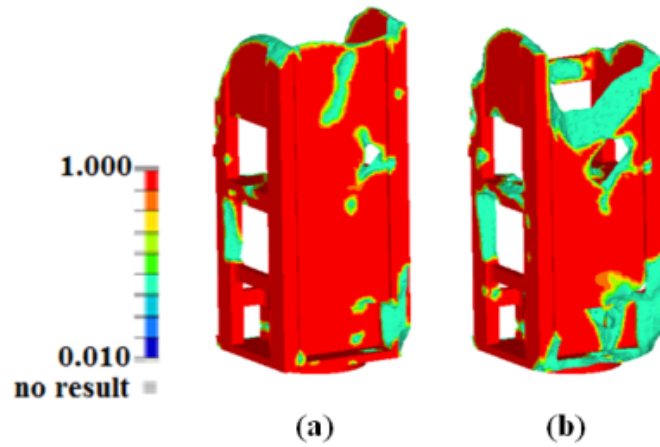
Fig. 23 (a) Spindle Head Top. Opt. for Model 1, (b) Spindle Head Top. Opt. for Model 2

On the contrary, local displacements are transmitted with two linear guides at sliding carriage and ram. Hence, there is considerably less volume fraction intensity at these local displacement areas in Model 2. The differences between the models can be seen more clearly in Fig. 24 and 25.
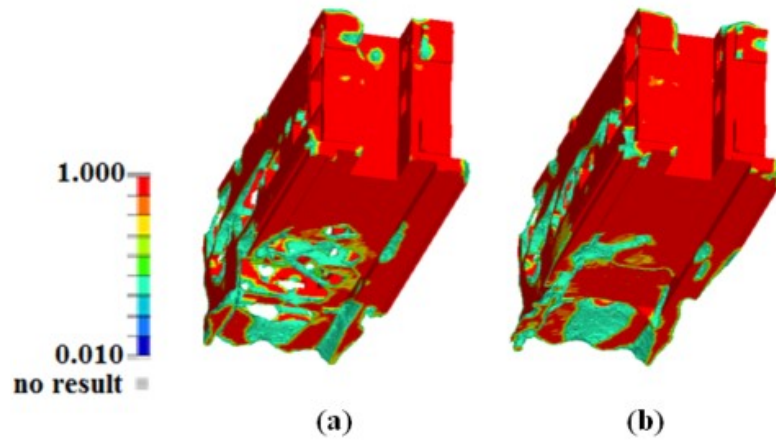
Fig. 24 (a) Ram Top. Opt. Model 1, (b) Ram Top. Opt. for Model 2
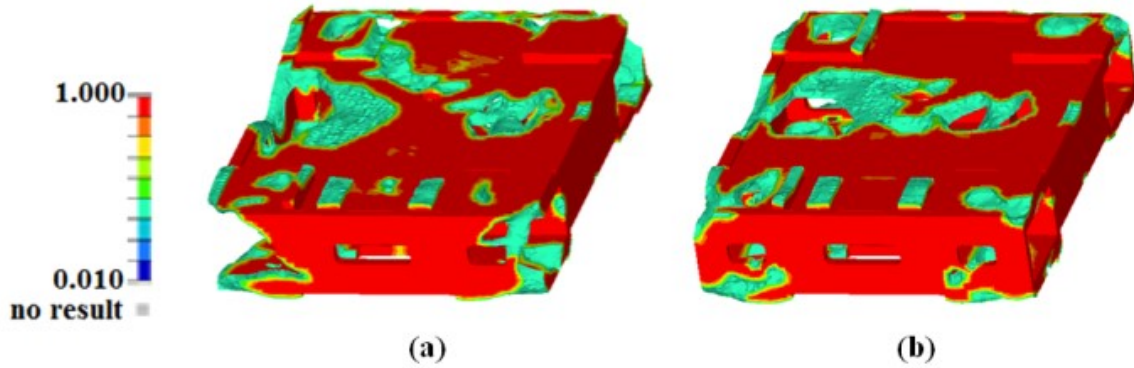
Fig. 25 (a) Sliding Car Top. Opt. for Model 1, (b) Sliding Car Top. Opt. for Model 2

The difference in topology causes different modal behaviors in Model 1 and 2. The change of modal behavior of the models is shown in Fig. 11 for 30% volume fraction.
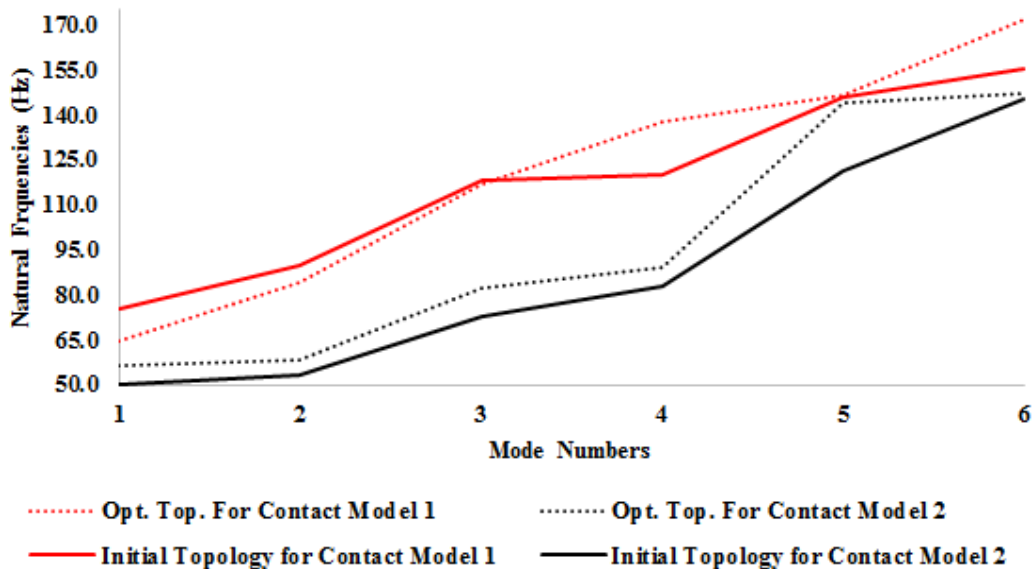
Fig. 26 Comparison of Natural Frequencies of Given Initial Design and Optimized Design

Fig.26 reveals that all the modes are shifted 10% for Model 2, but this trend is fluctuated for Model 1, and it is hard to predict modes behavior previously before the mass reduction. The difference in the predicted modes is around 40% between these two models. It is noteworthy that for an ordinary servo driver the first mode is around 45-60 Hz. For instance, Kroll and et al. [1], showed that the first mode of a Siemens drive (1FT6086-8AF7x model) is 44.8Hz. After 30% mass reduction, and by increasing the gains, the natural frequency shifted to 58.5

50

Hz. Thus, bandwidth of the dynamic control was extended for the corresponding axis. Therefore, they operate the drivers at higher angular frequencies easily. The importance of this example is, although different configurations of the assemblies, the first natural frequencies of the machine tool structure and the drivers are in a similar bandwidth. Hence, unrealistic representation of the linear guides, possibly will lead the overlapped modes at low frequencies and then, the gains must be limited at feed drives to defeat this situation. In other words, the highest angular frequencies will be limited and reaching upper limits for the drivers will not be possible.

4.5. Increased Stiffness Results for Model 2

In this section, effects of using stiffer linear guides are investigated at assembly level by focusing on topology optimization for early design stage predictions. Therefore, the new proposed virtual linear guide representation (Model 2) is employed for rolling elements to simulate full-assembly of the CNC structure. Reliability of the Model 2 were verified with static and dynamic experiments before. The comparison is done in the FE environment for the same topology algorithm that used before by increasing the stiffness of the contact elements.

Verified by the experiments, Model 2 provides precise results as the entire model behavior depends on the least stiff component. Based on this, the effect of linear guide stiffness is demonstrated within this study. The rolling elements' stiffness is increased 20%, under the same loading conditions. The iterative volume fraction process is repeated to explore mass reduction capacities of the given five-axis milling machine. The optimizations are performed with increasing volume fraction rate from 20% to 40%. For the greater volume fraction rate than 40%, the allowed displacement constraints are violated. The obtained structure for increased stiffness with a 40% volume fraction is plotted in Fig 27.

51
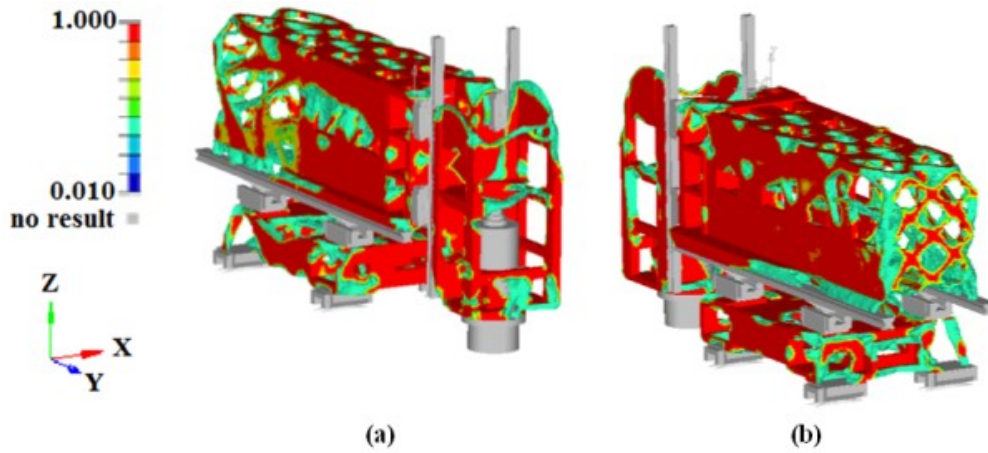
Fig. 27 Top. Opt. with %40 volume fraction for increased stiffness of the bearings; (a) Front View (b) Back View

It is noteworthy to remember, volume fraction rate was set to 20%, 25% and 30%, respectively in the optimization for stiffness values of the standard linear guides. It was seen that higher than 30% volume fraction rate caused violation of displacement constraints. However, volume fraction rate limits are 20% to 40% for the optimizations by 20% increasing the stiffness of the contact elements. This means that, nearly 20% stiffness increase in rolling element makes additional 10% volume reduction possible.

4.6. Comparison with the Original Stiffness
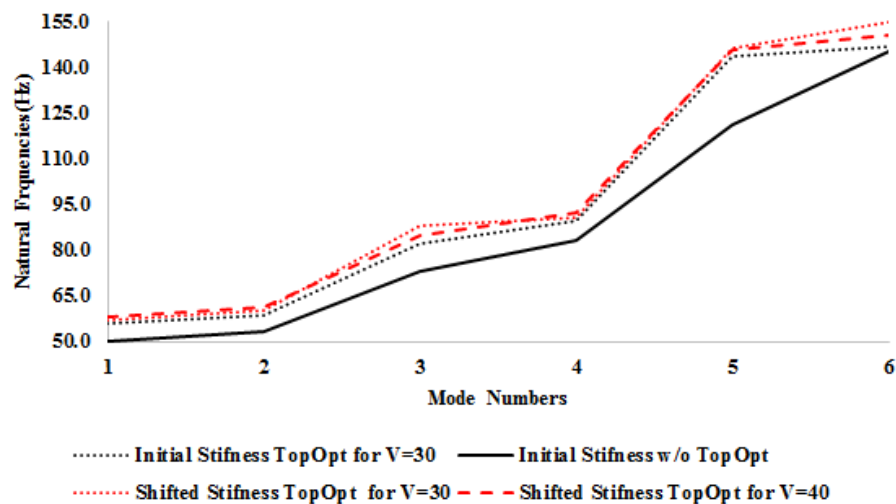
In this study, an extensive optimized topology comparison is presented by increasing roller elements stiffness of the liner guides in order to expose the possibilities extra mass reduction. The first six mode shapes are slightly changed for the optimized topologies. In Fig.28, the change of the mode shapes are displayed for the optimized topologies. The gap is nearly diminished between original stiffness and increased stiffness model results while the 10% additional volume fraction is posed to the model. This result is important, because it is possible to preserve the modal and static responses of the entire model while reducing mass by increasing stiffness of the linear guides. Thus, choosing stiffer linear guides is a much more effective way than creating massive structures for increasing global stiffness of the model.

Chapter 5 MULTIPLE-PHYSICS COMPARISON OF OPTIMIZED STRUCTURES WITH DIFFERENT LINEAR GUIDE REPRESENTATIONS

The static stiffness increase, organically affects dynamic and thermal characteristics of the machine tools' structural elements and joints. These joint element's effect on a machine tool structure is significant for the stiffness considerations. Up to now, maximum stiffness is considered as the objective for the CNC optimization application and rolling elements mentioned as the most flexible elements for the boundary conditions within the given design domain of machine tool structures.

On one hand, the employed topology optimization algorithm search the global optimum for the elasticity problem since the problem is convex and well-posed. The current topology optimization algorithm provides global optimum solutions for static stiffness which must be the major objective for machine tool designers. Unfortunately, dynamic and thermal behavior envision of the global optimization is not possible by employing gradient based algorithms therefore, as mentioned before heuristic methods have to be employed for local optimums.

On the other hand, it is obvious that, when static stiffness is improved, dynamic and thermal behaviors will be more satisfactory. The unknown side of this improvement is its' order. This information is significantly important to obtain the best possible machine tool design.

Another important point is knowing about approximate error percentage of FE simulations and topology optimizations due to unrealistic representation of linear guides at early design stage. Therefore, reliability of the optimization proposals are measured by crossing the equivalent linear guide representations for the proposed structures. Thus, Model 1 is selected as unrealistic representation for the linear guides while Model 2 is chosen as realistic representation for the linear guides. Same topology algorithm is employed for the both FE models. After this point, the topology optimization is executed by employing Model 1, and will be named as 'Contact-based Topology Optimization' while the other will be referred as 'Spring-based Topology Optimization' for ease of expression.

To be able to evaluate the dynamic and thermal improvement order with static optimization and to be able to measure error percentage due to unrealistic representation of the linear guide, the planned methodology is presented in Fig 29.
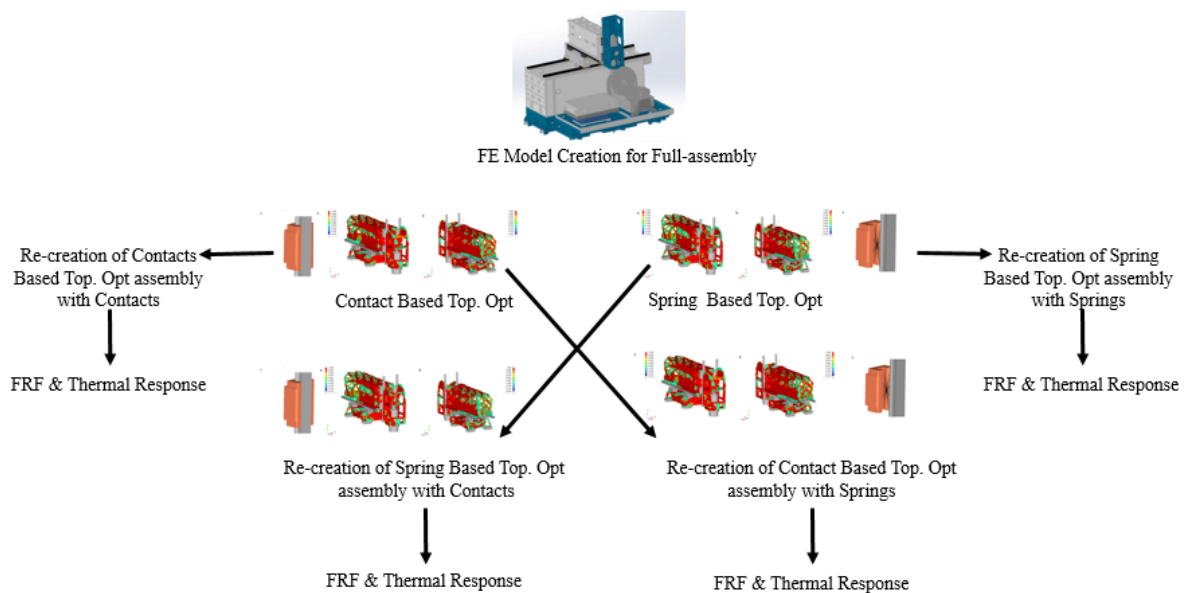

Fig. 29 Reliability measurement procedure of the optimization proposals by crossing the representations for the proposed structures

According to this procedure, an extensive Multiple-Physics comparison of different linear guide's representations is executed by crossing the representations for the proposed

structures, dynamically and thermally. First of all, dynamic behavior improvement and error percentage due to unrealistic representation will be investigated. Afterwards, the mentioned phenomenon will be searched for thermal behavior

5.1. Dynamic Comparison of Optimized Structures with Different Linear Guides Representations

In this section, an extensive dynamics comparison is presented to reveal the effects of realistic boundary conditions on min compliance topology optimization problem. Some optimized parameters contribute both static and dynamic characteristics for the min compliance problem. This positive contributors can be listed as the following;
-Shifting low structural modes to higher frequencies,
-Increase on stiffness characteristics.

 The first benefit refers energy efficiency due to lightweight design, because, first natural frequencies of structural modes and servo drives' modes are in a similar bandwidth and they are directly affected from each other. Therefore, the velocity gain, which is the main parameter for defining drive bandwidth, increases proportional to structural natural frequency. Thus, shifting natural frequencies to higher modes with an appropriate optimization problem statement provides double gain. Another important advantage is better process stability with mass reduction and stiffness increase at the same time.

To be able to benefit from all of the advantages, optimization problem statement and the employed algorithm are crucial for dynamics of the last design proposal. This benefits can be gained also from max frequency problem statement for a topology optimization application. Thus, min compliance problem and max frequency problem statement and solution algorithms compered in section 5.1.1 in order to obtain the best structures with shifted natural frequency. In section 5.1.2, static and dynamic compliance relation is expressed mathematically for the min compliance problem. Later, dynamic compliance comparison for different linear guide's representations is executed by crossing the representations of the linear guides for the optimized structures. Simulation errors are investigated in Section 5.1.3 due to unrealistic linear guide representation.

5.1.1. Comparison of Minimum Compliance & Maximum Frequency Problem Statement

The current topology optimization algorithm provide global optimum solutions by employing SIMP method and OC (Optimality Criteria) for static stiffness which must be the major objective for machine tool designs. Unfortunately, finding global optimum of dynamic behavior for a multimode system is not possible. Furthermore, even global maximization of a single eigenvalue is not guaranteed by employing the same solution methodology due to following reasons [2],

-The employed algorithm removes the entire structure to obtain an infinite eigenvalue, thus problem must be bounded.

-Even if the bounded problem is used, another pitfall is repeated eigenvalues. The repetitive eigenvalues are cannot differentiable by the employed algorithm.

-Eigenvalues behave asymmetric, they might be non-symmetric even the related structure is symmetric, but the employed algorithm uses symmetry features to reduce the problem size.

-Artificial modes might appear in low density loads which have relatively greater stiffness-mass ratio due to reconstructed material media by SIMP approach.

The most common dynamic optimization formulation is developed to obtain higher natural frequencies by maximizing the first smallest eigenvalue subject to a given amount of material. The dynamic problem can be formulated as the following for maximization of the smallest eigenvalue ($\lambda_{\min}$);

$$max_\rho = \{\lambda_{min} = min_{i=1,....Ndof} \quad \lambda_i\} \tag{12}$$

$$s.t. \quad (K - \lambda_i M)\varphi_i = 0, \quad i = 1,..,Ndof \tag{13}$$

$$\sum_{e=1}^{N} v_e \rho_e \leq V, \quad 0 < \rho_{min} \leq \rho_e \leq 1, \quad e = 1,..,N \tag{14}$$

Where **M** and **K** stand for the mass matrices and system stiffness, respectively while $\boldsymbol{\varphi}_i$ is associated eigenvector of ith element. As mentioned earlier, to avoid an absurd solution for infinite eigenvalues, an alternative bounded problem formulation can be stated as the following;

$$max_\rho = \beta \qquad (15)$$

$$s.t. \qquad \lambda_{\mathrm{i}} \le \beta \qquad (16)$$

$$(\boldsymbol{K} - \lambda_{\mathrm{i}}\boldsymbol{M})\boldsymbol{\varphi}_i = 0, \quad i = 1,..,Ndof$$

$$\textstyle\sum_{e=1}^{N} v_e\rho_e \le V, \quad 0 < \rho_{min} \le \rho_e \le 1, \quad e = 1,..,N$$

The eigenvalue objective has a lower bound which is indicated as λ_{i} in the problem statement, that can be the fundamental (1st mode) eigenvalue for the subjected structure. The pitfalls are not entirely considered within this problem statement, thus it is still required to improve for the repetitive eigenvalues. As a solution proposal, a percentage variable can be introduced to the problem which is indicated as α in the following problem formulation;

$$max_\rho = \beta \qquad (17)$$

$$s.t. \qquad [\alpha]^i\lambda_{\mathrm{i}} \le \beta$$

$$(\boldsymbol{K} - \lambda_{\mathrm{i}}\boldsymbol{M})\boldsymbol{\varphi}_i = 0, \quad i = 1,..,Ndof$$

$$\textstyle\sum_{e=1}^{N} v_e\rho_e \le V, \quad 0 < \rho_{min} \le \rho_e \le 1, \quad e = 1,..,N$$

Now, the problem statement is constrained intuitively due to the undesired issues related with the eigenvalues. Thus, search is not realistic anymore for the global optimum. Even though all the improvements, artificial modes risk continues due to SIMP interpolation of the material structure. Thus, instead of SIMP, heuristic evolutionary   methods must be employed.

Conversely, static minimum compliance problem is not needed any limitation due to its convenient nature. The minimum topology optimization formulation is developed to obtain

stiffer structure by minimizing the compliance subject to a given amount of material, [2]. Basically, minimizing compliance equals to minimizing the energy of deformation at the equilibrium state of the structure. This problem in weak form can be stated as the following by employing also SIMP approach in equations (20) and (21),

$$min_{u \in U, \rho} = \int_{\Omega} pu d\Omega + \int_{r_T} tu ds \tag{18}$$

$$s.t. \quad \int_{\Omega} C_{ijkl}(x) \varepsilon_{ij}(u) \varepsilon_{kl}(v) d\Omega = \int_{\Omega} pv d\Omega + \int_{r_T} tu dS, \quad \forall v \in U \tag{19}$$

$$C_{ijkl}(x) = \rho^p C_{ijkl}^0 \tag{20}$$

$$Vol(\Omega^m) = \int_{\Omega} \rho(x) d\Omega \leq V \quad 0 < \rho_{min} \leq 1, \tag{21}$$

$$Geo(\Omega^m) \leq K \tag{22}$$

Where, U denotes the space of kinematic admissible displacement regions, u is the equilibrium displacement, p is the body forces, t is boundary tractions, $\varepsilon(u)$ is the linearized strains, and $\rho(x)$ is the density, respectively. C_{ijkl} denotes the stiffness tensor of a given elastic material, whereas $Geo(\Omega^m)$ refers to limit geometry of the given domain Ω^m. V refers maximum limit of the admissible design volume.

As it can be seen from the weak form of the minimization problem, the problem statement is not extra constrained compared the dynamic problem statement due to its convenient nature. Thus, the employed minimum compliance topology optimization search the global optimum for an elasticity problem since the problem is convex and well-posed.

Minimization of Compliance	Maximization of Frequency
$min_{\rho} : \varphi(\rho) = F^T U$ $s.t.: \sum_{e=1}^{N} v_e \rho_e = v^T \rho \leq V^*, e = 1,..,N$ $: g_i(\rho) \leq g_i^*, \quad i = 1, ..., M$ $: 0 \leq \rho_{min} \leq \rho \leq 1$	$max_{\rho} : \{\lambda_{min} = min_{i=1,....Ndof} \ \lambda_i\}$ $s.t. \quad : (K - \lambda_i M) \varphi_i = 0, \quad i = 1,..,Ndof$ $: \sum_{e=1}^{N} v_e \rho_e \leq V,$ $: 0 < \rho_{min} \leq \rho_e \leq 1, \quad e = 1,..,N$

$w = \sqrt{\dfrac{k}{m}}$ Increased
          Reduced
	$w = \sqrt{\dfrac{k}{m}}$ Unknown
	          Reduced

Fig. 30 Comparison of Minimum Compliance Problem and Maximum Frequency Problem

Despite the differences described above, there is one important effect in common for both minimization compliance and maximum frequency problem: both ends with natural frequency increase. As reciprocal to natural frequency formulation, both problems ends with mass reduction, while minimization of compliance problem also comes with stiffness increase. But, finding stiffness increase for the maximum frequency problem is not known during the optimization stage. The stiffness value directly depends on eigenvalue solution which cannot guarantee stiffness improvement during the solution .Although this obstacle, solution for minimum compliance guarantees the highest stiffness value for a given amount of mass reduction. During the simulations, it is observed that the first six natural frequencies are shifted to higher modes by employing min. Compliance problem compared to max. Frequency problem. Fig. 31 interprets the natural frequency shifting results for both min compliance and max frequency problem statement by employing microstructure techniques for the same given amount of the material.
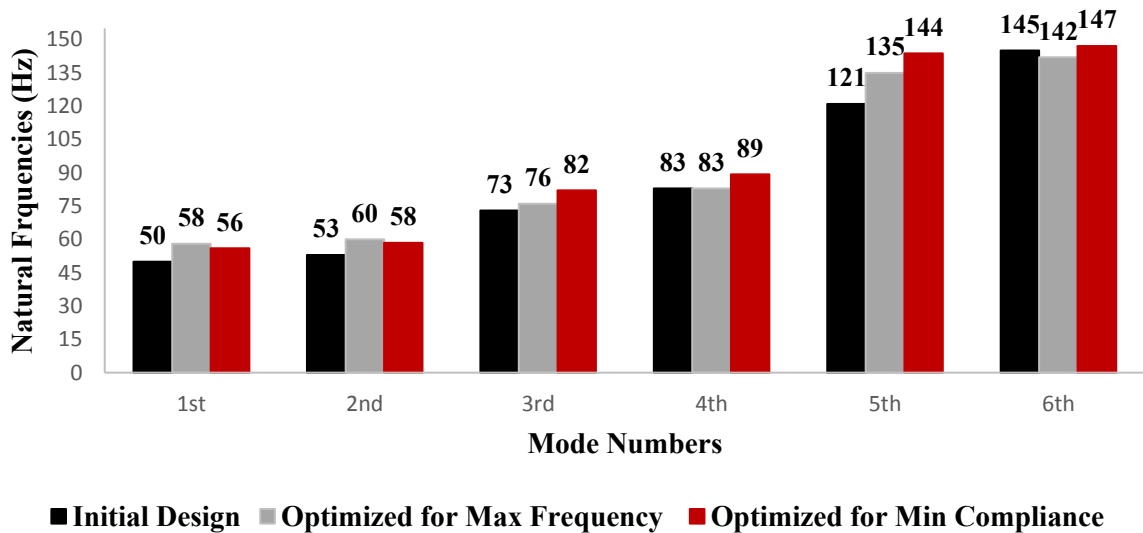

Fig. 31 Natural frequency shifts of Minimum Compliance Problem and Maximum Frequency for the same boundary conditions of the volume

5.1.2. Static & Dynamic Stiffness Relation for Minimum Compliance Optimization

The minimum compliance problem is stated in strong form before as the following,

$$min_\rho \; : \; \varphi(\rho) = \boldsymbol{F}^T \boldsymbol{U}$$

$$s.t. \; : \; \sum\nolimits_{e=1}^{N} v_e \rho_e = \boldsymbol{v}^T \boldsymbol{\rho} \; \leq \; V^*, e = 1, \dots, N$$

$$: \; g_i(\rho) \leq \; g_i^*, \;\; i = 1, \dots, M$$

$$: \; 0 \leq \; \rho_{min} \; \leq \rho \leq 1$$

$$: \; \boldsymbol{K}(\boldsymbol{\rho})\boldsymbol{U} = \boldsymbol{F}$$

Where, $\boldsymbol{K}(\boldsymbol{\rho})$ denotes the stiffness matrix while $\varphi(\rho)$ stands for the min compliance for the system, explicitly. It is noteworthy that, compliance is the measure of the strain energy in a continuum structure and its expression comes from bi-lateral energy formulation regulations. Thus, internal displacements drop with minimization of strain energy statically and dynamically. Hence, dynamic stiffness improvement is expected with minimization of the compliance, in other terms, with static stiffness maximization. The relation with stiffness and compliance is easily can be seen from the strong from of the optimization problem statement, if the equations are rearranged as the following;

$$\boldsymbol{\varphi} = \boldsymbol{F}^T \boldsymbol{U} \tag{23}$$

$$\boldsymbol{K} = \boldsymbol{F}\boldsymbol{U}^T \tag{24}$$

Thus, stiffness-compliance relation can be summarized approximately, as follows;

$$K = {}^1\!/_\varphi = {}^1\!/_{f_s} \tag{25}$$

It is obvious from the equation (25) compliance also can be referred as a measure of the flexibility of the system. Additionally, the flexibility term (f_s) can be used when the modal behavior is explained dynamically. Machine tool's structural dynamics can be evaluated by employing receptance frequency response method. The receptance term also called as 'dynamic compliance' which can be basically, formulated in Equation (26).

$$R = {}^u\!/_F \tag{26}$$

The transfer function of the receptance frequency response can be expressed by Equation (27).

$$R(w) = \frac{u}{F}(w) = \sum_{m=1}^{\infty}\left[\frac{f_m}{1-\left(\frac{w}{wn}\right)^2+2j\left(\frac{w}{wn}\right)^2\zeta_m}\right] \tag{27}$$

Where F denotes for the exciting force in the cutting force direction whereas u is the relative displacement at the given m[th] mode frequency of w. Viscous damping ratio stands with ζ_m for the mth natural mode within the problem formulation, while f_m denotes for the modal flexibility of the mth mode.

The static compliance equals receptence when w=0. Thus, the static flexibility can be expressed as the sum of modal flexibility in Equation (28).

$$f_s = \sum_{m=1}^{\infty} f_m \quad where \quad \forall w = 0 \tag{28}$$

Where f_s denotes static flexibility or compliance. The relation between static and dynamic compliance can be easily shown in Equation (29) by the rearranged Equation (28);

$$\sum_{m=1}^{\infty}(f_m/f_s) = 1 \tag{29}$$

f_m/f_s ratio is denoting here for the static contribution of the related m[th] mode. Additionally, it serves as function for flexibility stability of the natural modes. But most importantly, Equation (29) depicts relation with static compliance and dynamic compliance.

To sum up, the natural frequency shifting performance has been compared in the previous sub-section. The existence of the relation for the min compliance optimization and dynamic stiffness improvement is shown mathematically within this sub-section. Dynamic behavior improvement and error percentage due to unrealistic representation will be investigated in the next sub-section

5.1.3. Dynamic Compliance Comparison of Min Compliance Optimization Problem Due to Different Representation of Linear Guides

Firstly, a dynamic compliance evaluation is executed for different virtual linear guides representations which are introduced in Section 3, by crossing the Model 1&2 representations for the structural min compliance design proposals .Secondly, error percentage of FRF responses is investigated due to unrealistic representations of the linear guides' roller elements. Let's recall reliability measurement procedure of the optimization proposals by crossing the representations for the optimized structures for better understanding. A more focused reliability measurement procedure scheme is given in Fig. 32 specific to dynamics evaluation.
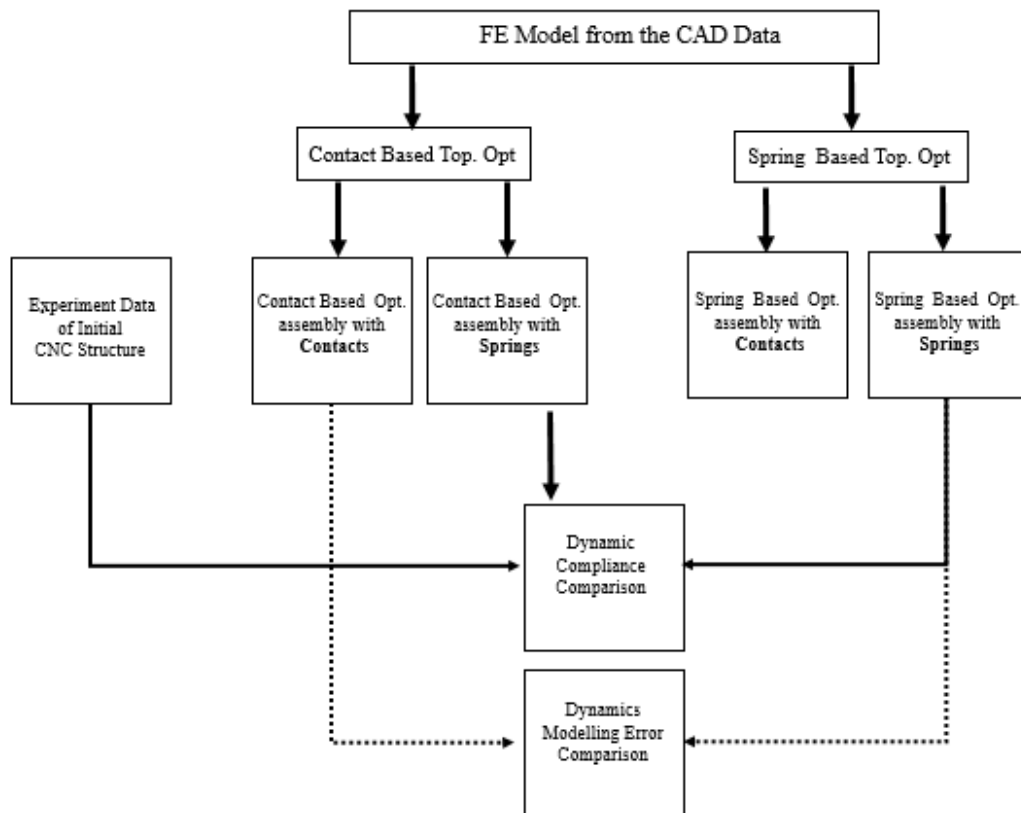

Fig. 32 Dynamic compliance evaluation procedure of the optimizations

Hammer tests which is introduced in Section 3, are conducted to measure the real FRF response for the initial CNC structure. As mentioned before, the experiments are designed to

measure FRF responses of the least stiff and most stiff position of the entire assembly. On one hand, Hammer Test 1 is conducted for the most rigid position of the CNC assembly. Thus, Y and Z axis are positioned at maximum limits of the machine tool whereas, Hammer Test 2 is conducted for the least rigid position of the CNC assembly. Hence, Y and Z axis are positioned at minimum limits of the machine tool. The same positioning policy is applied to the FE simulations of dynamic reliability measurement procedure in order to compare the differences are sourced from the linear guide representations.

5.1.3.1. Dynamic Compliance Comparison

5.1.3.1.1. Comparison for Most Rigid Position of the CNC Structure

FE simulations of contact based and spring based optimization design proposals are executed at Hammer Test 1 position by employing Model 2 (spring representation for linear guide rollers). Thus, Y and Z axis are positioned at maximum limits of the machine tool during the FE simulations. The simulation results are plotted in Fig. 33.

Fig. 33 FRF response comparisons of the FE simulations and Hammer Test 1 between 120 Hz-190 Hz

Fig.33 reveals that, spring-based optimization shifts natural modes to higher frequencies compared to contact-based optimization in the frequency range of interest. In addition, spring-based optimization offers ~25% better dynamic stiffness compared to contact-based one for the observed single mode during the experiment. This dynamic stiffness improvement is due to difference of the boundary conditions for the same topology algorithm.

64

To be able to obtain all the structural modes, frequency range is extended, thus simulations repeated between 10 Hz to 1000 Hz with 1 Hz increment. A multi-mode system, which is consist of four modes, is observed for the extended frequency range. The simulation results are illustrated in Fig. 34. All of the natural frequencies are shifted to higher modes, whereas the third mode shifted most for both of the topology optimization proposals. The third mode is again reported as the dominant mode during the Hammer test 1&2, thus its improvement is significant, because it is effected by moving components of the CNC structure.
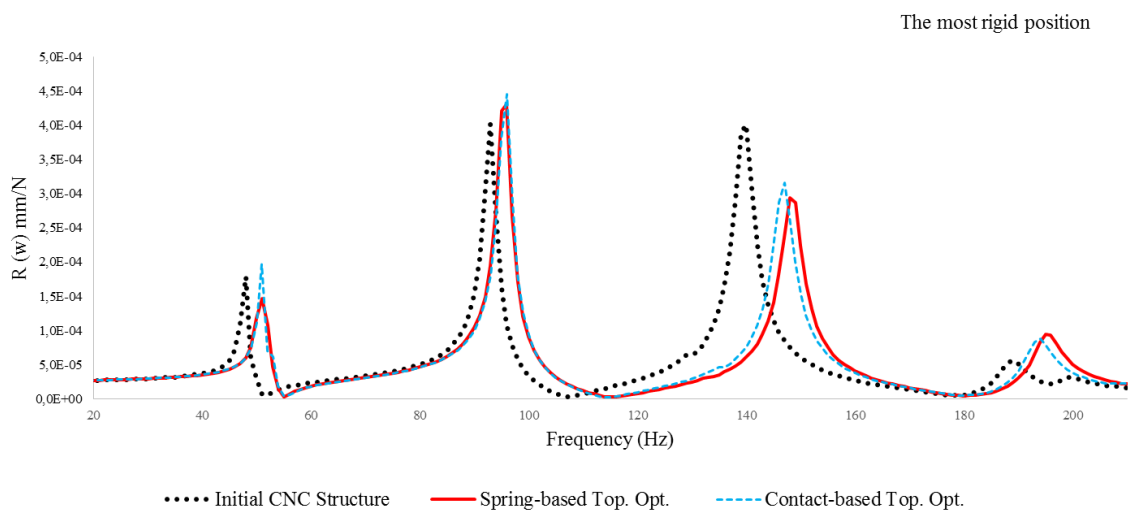
Fig. 34 FRF response comparisons of the FE simulations between 20 Hz-200 Hz

The first mode is nearly stable in terms of dynamic stiffness after 30% volume reduction for the contact-based optimization while its dynamic stiffness increase is ~15% compared the initial design. The dynamic stiffness is reduced by the two of the design proposals at the second mode. For the dominant mode of the system, dynamic stiffness improvement is ~25% for the both. The forth mode dynamic stiffness drops while natural frequencies shifts most for the spring-based optimization .Although this reduce, spring-based topology optimization performs better than contact-based topology optimization in overall.

5.1.3.1.2. Comparison for Least Rigid Position of the CNC Structure

FE simulations of contact based and spring based optimization design proposals are simulated at Hammer Test 2 position by employing Model 2 (spring representation for linear guide rollers). Thus, Y and Z axis are positioned at minimum limits of the machine tool during the FE simulations. The simulation results are plotted in Fig. 35.
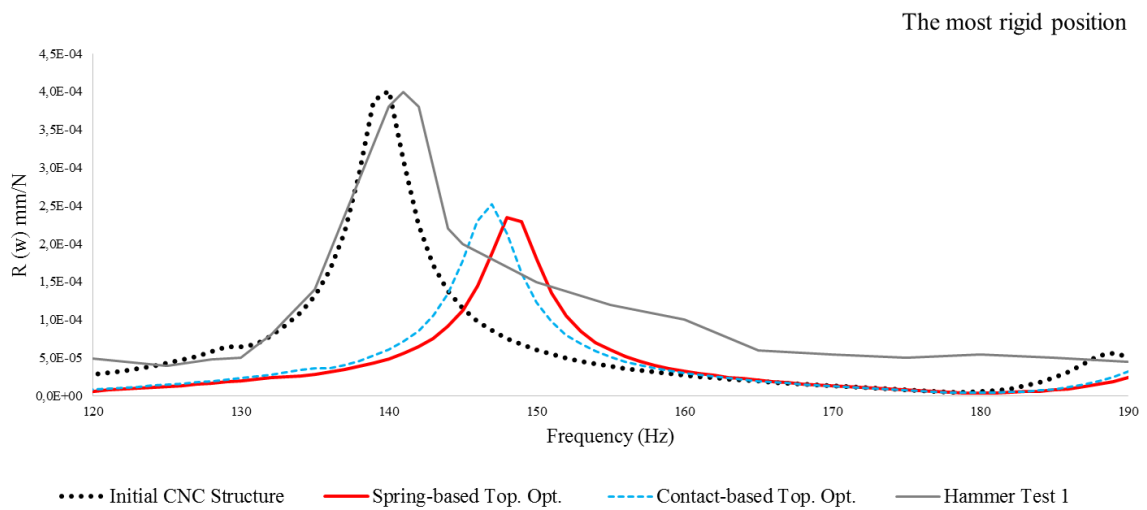
Fig.35 indicates that, contact-based optimization shifts natural modes to higher frequencies compared to the other optimization in the frequency range of interest. In addition, contact - based optimization offers ~20% better dynamic stiffness for the observed single mode during the experiment. This difference is sourced from the employed boundary conditions for the same topology algorithm.
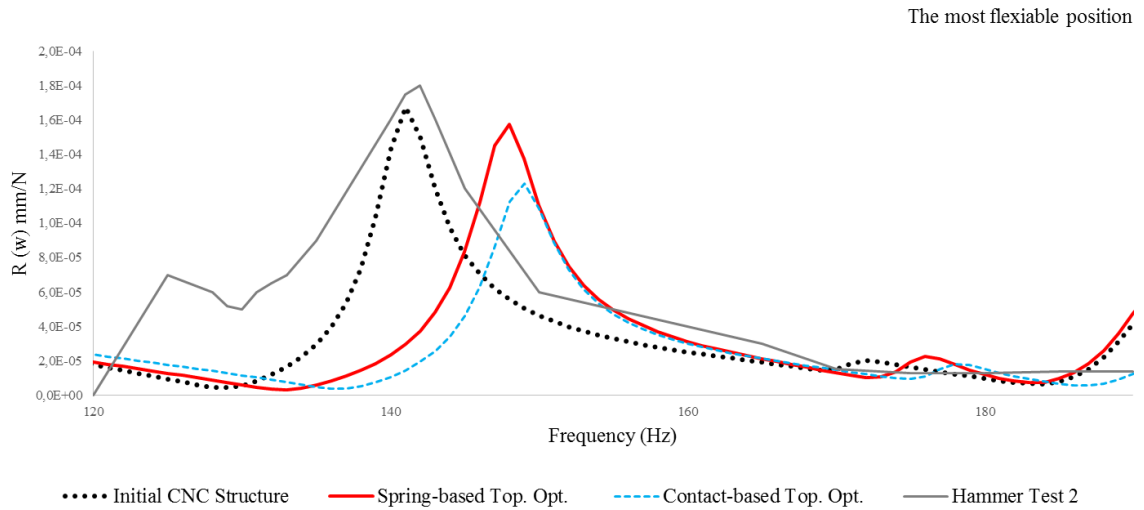
Fig. 35 FRF response comparisons of the FE simulations and Hammer Test 2 between 120 Hz-190 Hz

To be able to obtain all the structural modes, frequency range is extended again to 10Hz to 1000Hz with 1 Hz increment. A multi-mode system, which is consist of 2 dominant modes, is observed for the extended frequency range. The simulation results are illustrated in Fig. 36. All of the natural frequencies are shifted to higher modes, whereas the first mode shifted most for both of the topology optimization proposals.

66
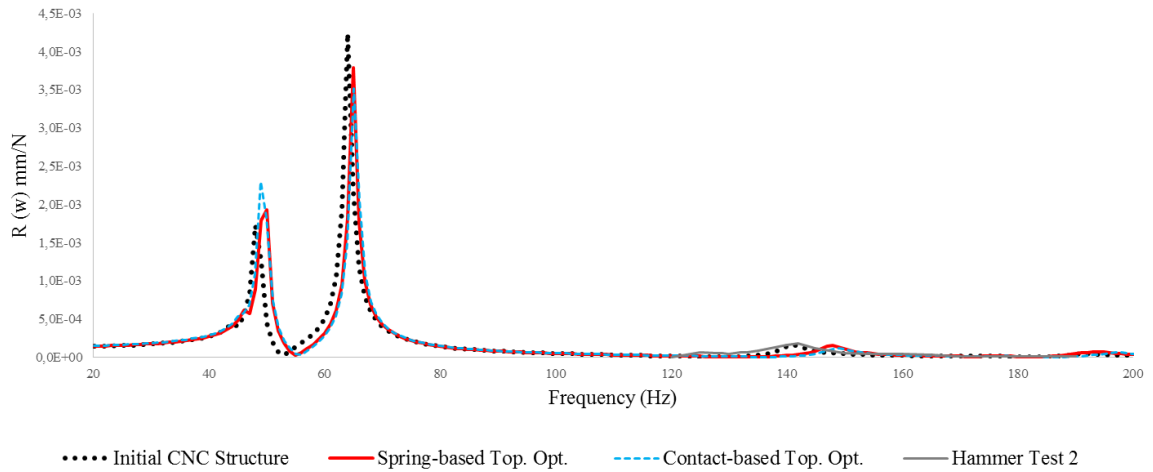
Fig. 36 FRF response comparisons of the FE simulations between 20 Hz-200 Hz

On one hand, dynamic stiffness stays the same for the first mode while, it is increased 25% by spring-based optimization compared the initial design. On other hand, dynamic stiffness drops for the first natural frequency of the contact-based design whereas, it is increased nearly same with spring-based contact at second mode.

It is also observed that the spring-based optimization design proposal performs better at the first natural frequencies of the assemblies for both most and least rigid positions. This is a remarkable solution when servo-drives considered, because they are in similar bandwidth for the first natural frequencies.

5.1.3.1.3. Dynamics Modelling Error Comparison

Dynamic compliance evolution is demonstrates for Hammer Test 1 position in order to depict the error parentage as the effect of the linear guide's unrealistic representation by employing Model 1 during the optimization .FE simulation results are plotted in Fig. 37 for the initial models and design proposals.
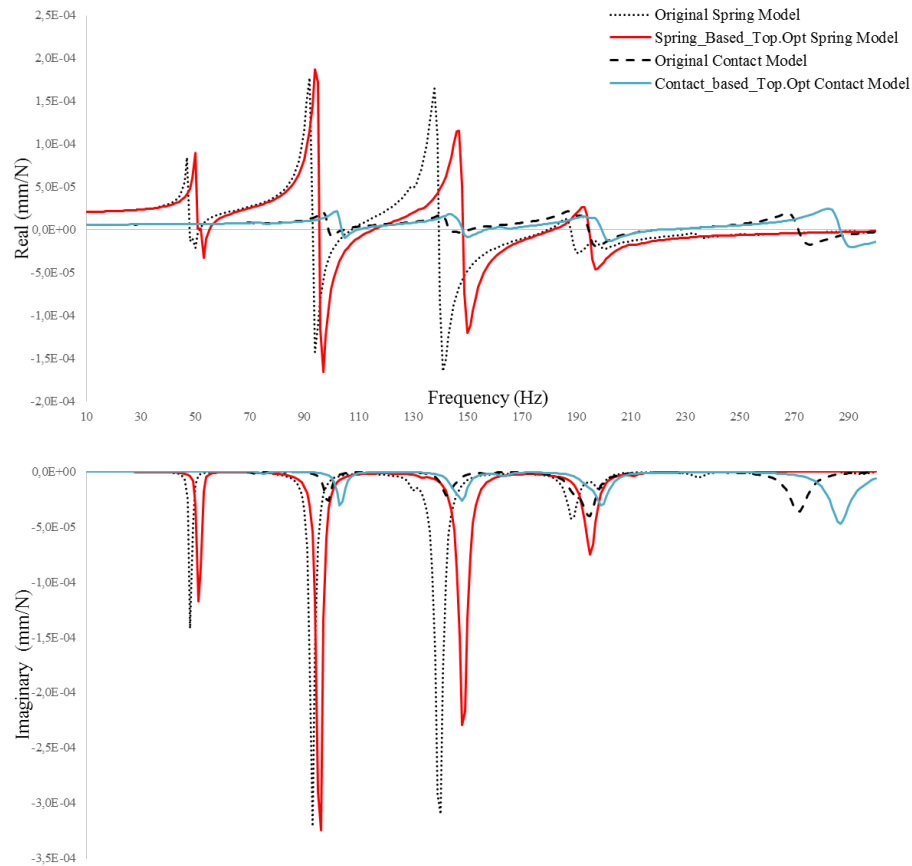
Fig. 37 FRF response evaluations of the FE simulations between 10 Hz-200 Hz

Fig. 37 clearly indicates that, natural frequencies are predicted more than 50% wrong for design proposals and initial models by employing Model 1. Response functions magnitudes are predicted at least more than 8 times for real part, where as it is more than 2 times for the imaginary part.

5.2. Thermal Comparison of Optimized Structures with Different Linear Guide Representations

As mentioned previously, min compliance equals to minimum energy amount of deformation at the equilibrium state of the structure. Thus, thermal and static displacement can be coupled by regularizations of bilateral energy formulations, to search for the global optimum. For the mentioned coupling, the min compliance problem can be stated as the following by

68

introducing a new thermal strain sensor which is indicated in Equation (31) for a linear elasticity problem [30].

$$min_{u \in U, \rho} = \int_{\Omega} pu d\Omega + \int_{r_T} tu ds$$

$$s.t. \quad \int_{\Omega} C_{ijkl}(x)\alpha_{ij}(u_{\rho 2})\varepsilon_{ij}(u_{\rho 1})\varepsilon_{kl}(v)d\Omega = \int_{\Omega} pv d\Omega + \int_{r_T} tu dS, \quad \forall v \in U \qquad (30)$$

$$\alpha_{ij} = (1 - \rho 2^p)\alpha_{ij}{}^1 + \rho 2^p \alpha_{ij}{}^2 \qquad (31)$$

$$C_{ijkl}(x) = \rho^p C^0_{ijkl}$$

$$Vol(\Omega^m) = \int_{\Omega} \rho(x)d\Omega \leq V \quad 0 < \rho_{min} \leq 1,$$

$$Geo(\Omega^m) \leq K$$

Where $\rho 1$ stands for artificial density for the SIMP method of the min static compliance problem while $\rho 2$ denotes for 'the new thermal density of the artificial media' which is completely discrete from $\rho 1$.

The main problem within this problem formulation is boundaries. The boundaries must be well-posed and these boundaries requires special conditions types for conduction such as Hashin-Shtrikman bounds [24] and also requires new penalization number technics such as RAMP etc. [42]. Fig 39 demonstrates the boundaries and penalization number techniques importance during the min compliance problem by employing SIMP approach [42].
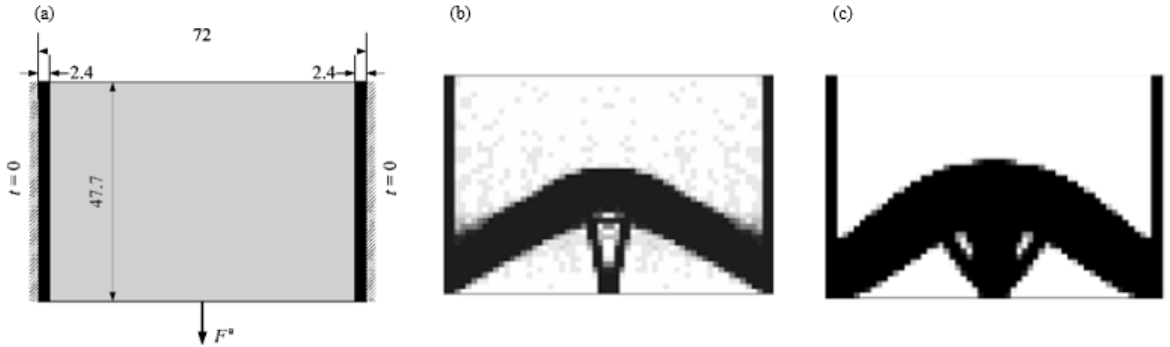
Fig. 38 (a) Initial design with loading (b) Optimized design with SIMP method (ΔT = 3°C) (c) Well-bounded optimized design with RAMP method (ΔT = 3°C) [42]

Fig. 38 depicts the effect of the bounds and penalization during the thermal coupled min compliance problems. In addition, homogenization of the composite media is crucial for topology optimization of thermal-elastic and electromagnetic based solutions. For instance

by using homogenization techniques , an extreme thermally expandable microstructure designed by Sigmund &Torquato via the topology algorithm which is based on interpolation of thermal strain tensor density [30].

The given examples on above part proves the importance of the boundary conditions when the min compliance problem coupled with thermal displacements. Thus, a better thermo-elastic performance can be expected when the boundary conditions became well-posed. Therefore, realistic virtual representation of linear guides must have a significant effect on topology optimization due to realistic boundary conditions of the least stiff elements when thermal considerations are taken into account. In order to investigate the mentioned effect, a thermal reliability measurement procedure is developed by crossing the virtual linear guide's representations which are proposed before in Section 3. According the thermal reliability measurement procedure, two situations are considered as indicated below,
- The thermal gradient change in the room during day time.
-The heat produced by high speed applications from the spindle bearings.

The thermal reliability scheme is interpreted in Fig. 39 for better visualization. The main purpose is to compare thermal performance of the machine tool for the spring-based and contact-based topology optimization.
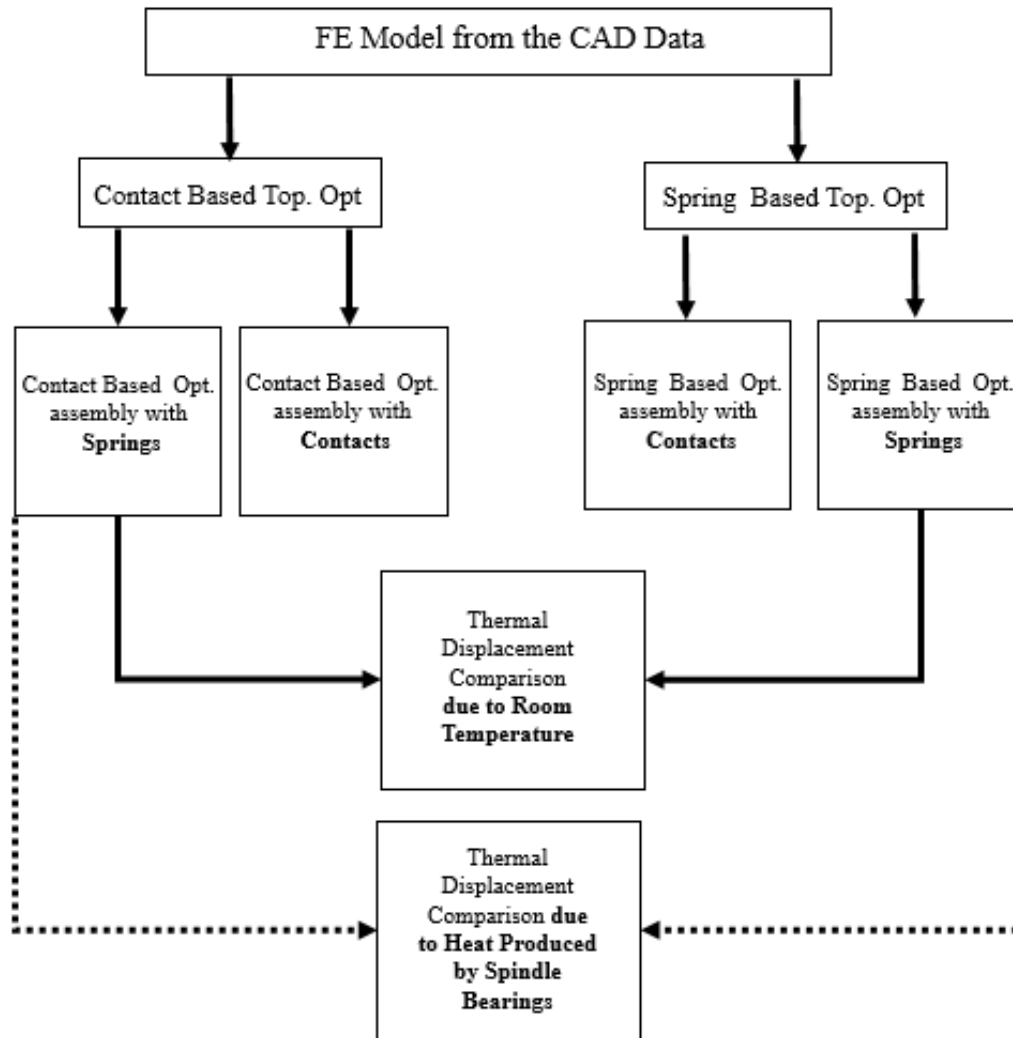
Fig. 39 Thermal reliability measurement procedure

5.2.1. Thermal Comparison Due to Room Temperature Change

Production shop-floors temperature is not steady during day and night time, and most of the time, there is no special consideration to keep stable the manufacturing facility temperature due to expensive air conditioning costs. In addition, windows position are not taken into account for the CNC structures, when they are located. However, its position might have crucial matter on the machining performance for the parts with narrow tolerances especially when the facility walls made from metal composites for prefabs. Thus, a thermal gradient change is investigated in the room temperature for the CNC design comparisons of the spring-based and contact-based optimizations. According the employed scenario, temperature

gradient varies 18 C to 24 C from the front facade to the back side of the CNC by considering a window located at back side at noon. FE simulations are run for the both spring-based and contact-based design proposals by employing Model 2 as linear guide representation. The results are tabulated in Table 6.

Table 6 Thermo-elastic displacement comparison due to room temperature change for spring-based and contact-based design proposals

FE Models	Simulated Maximum Displacement
Initial Model	2,75 μm
Contact-based Optimized	3,04 μm
Spring-based Optimized	2,33 μm

Table 6 proves again the significance of boundary conditions for topology optimization when thermal considerations taken into account even for a pure min compliance problem. According to findings contact-based optimization offers designs with low thermal performance compared to spring-based optimization. In one hand, thermo-elastic displacement increased by 10% compared to initial design of the subjected CNC. On the other hand, 15% thermal performance improvement is observed for the spring-based optimization.

5.2.2. Thermal Comparison Due to Heat Produced by Spindle Bearings

As stated in the current literature before many times, spindle bearings are the most important heat producers due to friction which occurs at high speeds. Thus, the heat amount is calculated for different spindle speeds, and its effect is investigated for the CNC design comparisons of the spring-based and contact-based optimizations. As the keynote, FAG HC 7011 type spindle bearings are employed for the subjected five-axis CNC (Spinner U1520).

The values of the heat produced by spindle bearings are plotted before by Yalçın [43] as indicated in Fig. 40.
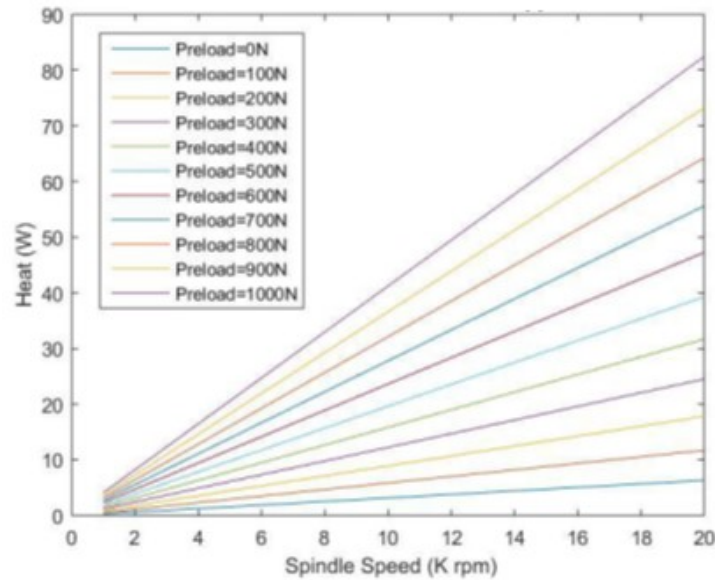
Fig. 40 The heat values for FAG HC 7011 type spindle bearings at different spindle speeds [43]

According the employed scenario, the heat values are taken for 10K rpm and 20K rpm with 500 N preloading [43]. FE simulations are run for the both spring-based and contact-based design proposals by employing Model 2 as linear guide representation. The results are tabulated in Table 7.

Table 7 Thermo-elastic displacement comparison due to heat generation at high spindle speeds

FE Models	Max Disp. at 10 K rpm	Max Disp. at 20K rpm
Initial Model	2,45 μm	2,56 μm
Contact-based Optimized	2,87 μm	3,30 μm
Spring-based Optimized	2,01 μm	2,50 μm

Table 7 reveals again the significance of boundary conditions for topology optimization when thermal considerations are taken into account. According to findings, contact-based optimization offers designs with low thermal performance compared to spring-based optimization. Thermo-elastic displacement increased by 17% compared to initial design of the subjected CNC for the contact-based optimization. On the other hand, 18% thermal performance improvement is observed for the spring-based optimization for 10K rpm.The true boundary conditions representation become more significant when the spindle speed are on the top limits. According to findings, contact-based optimization offers designs with low thermal performance compared to spring-based optimization for 20K rpm spindle. In one hand, thermo-elastic displacement increased by 29% compared to initial design of the subjected CNC for contact -based optimization. On the other hand, 2% thermal performance improvement is observed for the spring-based optimization.

Chapter 6 **CONCLUSIONS**

6.1. Conclusions

In this study, the importance of accurate modeling of linear guides is presented for modeling entire assembly for machining centers in order to obtain lightweight structures. According to static and dynamic reliability tests, spring-based representation (Model 2) gives much more trustable results compared the contact-based roller representation (Model1).

Effects of bearing and interface parameters on the modes and on the displacements are analyzed and vital conclusions are derived for topology optimization applications:

- The rolling elements in the linear guides are significant during the process of FE modeling in virtual environment. Representing them directly by employing Model 2 in the virtual environment gives realistic predictions. Moreover, realistic prediction of structural modes prevents feed drives running bandwidth limitations at early design stage. In this way, reaching upper limits for the drivers will be possible for lightweight machining centers.
- Restricting maximum deflection as a topology optimization constraint gives the same result for spindle tip and for the other moving components.
- Choosing stiffer linear guides is a much more effective way than creating massive structures for increasing global stiffness of the model. By employing this approach, it is possible to preserve the modal and static response of the entire structural model while reducing mass and by increasing the stiffness of the linear guides.

75

Additionally, a multi-physic comparison is investigated for realistic and unrealistic boundary conditions at multi-component level optimization applications. It is obviously observed that, optimization for minimum compliance also contributes minimization of the dynamic compliance with the true and realistic boundary conditions which are equals linear guides for moving bodies at machining centers. The same optimization also contributes the minimization of thermos-elastic displacements with the realistic boundary conditions at multi-component level.

The dynamic stiffness is increased approximately ~20%, whereas this contribution is around ~15% for thermal stiffness with proper boundary conditions. Thus, only changing the material removal location affects structural dynamics and thermal behavior remarkably with true boundary conditions.

This conclusions may not be generalized for the all machining center configurations, but they can give an insight into FE model creation and topology optimization process and the importance of linear guide's representation.

6.2. Contributions

The contributions are listed as the following,

- A novel 3-D linear guide representation method by employing 1-D springs is presented. The reliability of the proposed method is verified via static and dynamic experiments.

- Effects of accurate linear contact representation of machine tools is demonstrated on topology optimization. Thus, realistic boundary conditions importance is proved for multi-component level topology optimizations of machine tool structures. The results have been shared as a publication in 17th CIRP conference with the title of *'The Effect of Linear Guide Representation for Topology Optimization of a Five-axis Milling Machine' [34].*

- As the last, it is proved that minimum compliance problem contributes dynamic and thermal stiffness with proper boundary conditions for multi-component level topology optimization applications. A five-axis milling machine specific comparison is executed within this study.

6.3. Future Work

The machine tools potentials are listed for topology optimization the as the following,

- An extensive thermal comparison are being studied for realistic boundary conditions specific to the subjected five-axis CNC. The conclusions will be shared at 8th UTIS conference with the title of *'A Thermal Structure Optimization Methodology by Including Contact Parameters for Machine Tools'.*
- A dynamic compliance problem might be stated by using static & dynamic compliance ratio for the employed minimum compliance problem. The solution might be semi-analytic for the mentioned problem statement.
- The proposed linear guide representation might be used for the topology optimization methodologies and software special for machine tools.

BIBLIOGRAPHY

[1] Kroll, L., Blau, P., Wabner, M., Frieß, U., Eulitz, J., & Klärner, M. (2011). Lightweight components for energy-efficient machine tools. CIRP Journal of Manufacturing Science and Technology, 4(2), 148-160.

[2] Bendsoe, M. P., & Sigmund, O. (2013). Topology optimization: theory, methods, and applications. Springer Science & Business Media.

[3] Dadalau, A., Groh, K., Reuß, M., & Verl, A. (2012). Modeling linear guide systems with CoFEM: equivalent models for rolling contact. Production Engineering, 6(1), 39-46.

[4] Ertürk, A., Özgüven, H. N., & Budak, E. (2007). Effect analysis of bearing and interface dynamics on tool point FRF for chatter stability in machine tools by using a new analytical model for spindle–tool assemblies. International Journal of Machine Tools and Manufacture, 47(1), 23-32.

[5] Altintas, Y., Brecher, C., Weck, M., & Witt, S. (2005). Virtual machine tool. CIRP Annals-manufacturing technology, 54(2), 115-138.

[6] Budak, E., Ertürk, A., & Özgüven, H. N. (2006). A modeling approach for analysis and improvement of spindle-holder-tool assembly dynamics. CIRP Annals-Manufacturing Technology, 55(1), 369-372.

[7] Law, M., Altintas, Y., & Phani, A. S. (2013). Rapid evaluation and optimization of machine tools with position-dependent stability. International Journal of Machine Tools and Manufacture, 68, 81-90.

[8] Luo, T., Wang, C., Liang, S. (2016). A Process Stability Enhanced Machine Tool Design Method Integrated Dynamic Stiffness Topology Optimization. The 17th International Conference on Machine Design and Production.

[9] Lee, E., James, K. A., & Martins, J. R. (2012). Stress-constrained topology optimization with design-dependent loading. Structural and Multidisciplinary Optimization, 46(5), 647-661.

[10] Sørensen, S. N., & Stolpe, M. (2015). Global blending optimization of laminated composites with discrete material candidate selection and thickness variation. Structural and Multidisciplinary Optimization, 52(1), 137-155.

[11] Zuo, K. T., Chen, L. P., Zhang, Y. Q., & Yang, J. (2006). Manufacturing-and machining-based topology optimization. The International Journal of Advanced Manufacturing Technology, 27(5-6), 531-536.

[12] Zhou, M., Fleury, R., Shyy, Y. K., Thomas, H., & Brennan, J. M. (2002, September). Progress in topology optimization with manufacturing constraints. In Proceedings of the 9th AIAA MDO conference AIAA-2002-4901.

[13] Law, M., Phani, A. S., & Altintas, Y. (2013). Position-dependent multibody dynamic modeling of machine tools based on improved reduced order models. Journal of Manufacturing Science and Engineering, 135(2), 021008.

[14] Weule, H., Fleischer, J., Neithardt, W., Emmrich, D., & Just, D. (2003, June). Structural Optimization of Machine Tools including the static and dynamic Workspace Behavior. In The 36th cirp-international seminar on manufacturing systems (Vol. 12, pp. 56-60).

[15] Engin, S., & Altintas, Y. (2001). Mechanics and dynamics of general milling cutters.: Part I: helical end mills. International Journal of Machine Tools and Manufacture, 41(15), 2195-2212.

[16] M. Albayrak, T. K. Yalcin, M. Erberdi, E. Ozlu, E. Budak (2015). Static and Dynamic Analysis of Different Machine Tool Spindles. 8th International Conference and Exhibition on Design and Production of MACHINES and DIES/MOLDS

[17] Neugebauer, R., et al, 2010, Structure Principles of Energy Efficient Machine Tools. 1, Internationales Kolloquium eniPROD (24–25.06.2010, Chemnitz).

[18] Cho, S.K., Kim, H.J., Chang, S.H., 2011, The Application of Polymer Composites to the Table-top Machine Tool Components for Higher Stiffness and Reduced Weight, Composite Structures, 93:492–501.

[19] Bang, K.G., Lee, D.L., 2002, Design of Carbon Fibre Composite Shafts for High Speed Air Spindles, Composite Structures, 55/February (2): 247–259.

[20] EU, Ecodesign Directive 2006/32/EG

[21] Altintas, Yusuf. Manufacturing automation: metal cutting mechanics, machine tool vibrations, and CNC design. Cambridge university press, 2000.

[22] Sencer, B., Altintas, Y., & Croft, E. (2009). Modeling and control of contouring errors for five-axis machine tools—part I: modeling. Journal of Manufacturing Science and Engineering, 131(3), 031006.

[23] K. Erkorkmaz, Y. Altintas, Trajectory generation for high speed milling of molds and dies, Proceedings of the Second International Conference and Exhibition on Design and Production of Dies and Molds, Kusadasi, Turkey, DM_46 2001

[24] Bendsøe, M. P., & Sigmund, O. (1999). Material interpolation schemes in topology optimization. Archive of applied mechanics, 69(9), 635-654.

[25] Yoshimura, M. (2007). System design optimization for product manufacturing. Concurrent Engineering, 15(4), 329-343.

[26] Eschenauer, H. A., & Olhoff, N. (2001). Topology optimization of continuum structures: a review. Applied Mechanics Reviews, 54(4), 331-390.

[27] Bendsøe, M. P., & Kikuchi, N. (1988). Generating optimal topologies in structural design using a homogenization method. Computer methods in applied mechanics and engineering, 71(2), 197-224.

[28] Guedes, J., & Kikuchi, N. (1990). Preprocessing and postprocessing for materials based on the homogenization method with adaptive finite element methods. Computer methods in applied mechanics and engineering, 83(2), 143-198.

[29] Tenek, L. H., & Hagiwara, I. (1994). Optimal rectangular plate and shallow shell topologies using thickness distribution or homogenization. Computer methods in applied mechanics and engineering, 115(1), 111-124.

[30] Sigmund, O., & Torquato, S. (1997). Design of materials with extreme thermal expansion using a three-phase topology optimization method. Journal of the Mechanics and Physics of Solids, 45(6), 1037-1067.

[31] Xie, Y. M., & Steven, G. P. (1993). A simple evolutionary procedure for structural optimization. Computers & structures, 49(5), 885-896.

[32] Young, V., Querin, O. M., Steven, G. P., & Xie, Y. M. (1999). 3D and multiple load case bi-directional evolutionary structural optimization (BESO). Structural and Multidisciplinary Optimization, 18(2), 183-192.

[33] Rozvany, G. I. (2009). A critical review of established methods of structural topology optimization. Structural and multidisciplinary optimization, 37(3), 217-237.

[34] Yüksel, E., Budak, E., & Ertürk, A. S. (2017). The Effect of Linear Guide Representation for Topology Optimization of a Five-axis Milling Machine. Procedia CIRP, 58, 487-492.

[35] Altintas, Y., & Cao, Y. (2004). A general method for the modeling of spindle-bearing systems. J. of Mechanical Design, 126-6.

[36] Kikuchi, N., & Oden, J. T. (1988). Contact problems in elasticity: a study of variational inequalities and finite element methods. Society for Industrial and Applied Mathematics.

[37] http://www.spinner.com.tr/urunler/16/u-1520-serisi.html

[38] https://www.boschrexroth.com/en/us/products/product-groups/goto   products/goto-linear-motion/ball-rails/standard-runner-blocks/index

[39] Dadalau, Alexandru, et al. "Modeling linear guide systems with CoFEM: equivalent models for rolling contact." Production Engineering 6.1 (2012): 39-46.

[40] Polycarpou, A. A., and Etsion, I., 1999, ''Analytical Approximations in Modeling Contacting Rough Surfaces,'' ASME J. Tribol., 121, pp. 234–239

[41] Polycarpou, A. A. (2005). Measurement and modeling of normal contact stiffness and contact damping at the meso scale. Journal of vibration and acoustics, 127(1), 52-60.

[42] Gao, T., & Zhang, W. (2010). Topology optimization involving thermo-elastic stress loads. Structural and multidisciplinary optimization, 42(5), 725-738.

[43] Yalçın,T.K. (2015) Thermal Modelling Of High Speed Machine Tool Spindles-Master Thesis-Sabanci University